Reaction Mechanism About Isomerization of Resin Acids and Synthesis of Acrylopimaric Acid Based on DFT Calculation

Wu-Ji Lai
Guangxi University for Nationalities
Jia-Hao Lu
Guangxi University for Nationalities
Rui Jiang
Beijing Huadian Tiande Assets Management Co Ltd Beijing Key Laboratory of High Voltage and Electromagnetic Compatibility
Lei Zeng
Guangxi University for Nationalities
Ai-qun Wu
Guangxi University for Nationalities
liqun shen (liqunshen@126.com)
Guangxi University for Nationalities

Research Article

Keywords: DFT, acrylopimaric acid, reaction mechanisms

Posted Date: December 21st, 2021

DOI: https://doi.org/10.21203/rs.3.rs-1108915/v1

Reaction mechanism about isomerization of resin acids and synthesis of acrylopimaric acid based on DFT Calculation

Wu-Ji Lai[a], Jia-Hao Lu[a], Rui Jiang[c], Lei Zeng[a], Ai-qun Wu[a], Li-Qun Shen[a,b] *

([a] College of Chemistry and Chemical Engineering, Guangxi University for Nationalities, Key Laboratory of Chemistry and Engineering of Forest Products, State Ethnic Affairs Commision, Guangxi Key Laboratory of Chemistry and Engineering of Forest Products, Guangxi Collaborative Innovation Center for Chemistry and Engineering of Forest Products, Nanning 530006, People's Republic of China. [b]GuangXi Key Laboratory of Zhuang and Yao Ethnic Medicine, Nanning 530006, People's Republic of China. [c]China Huadian Group Guigang Power Co., Ltd, Guigang, 537100, People's Republic of China.)

Correspondence: Liqun Shen, College of Chemistry and Chemical Engineering, Guangxi University for Nationalities, Nanning 530006, People's Republic of China. Email liqunshen@126.com

ABSTRACT

Acrylopimaric acid is considered one of the possible substitutes for petroleum-based polymeric monomers, which is an important industrial product. Resin acids were isomerized to form levopimaric acid(4), which reacted with acrylic acid to synthesize isomers of acrylopimaric acid. Density functional theory calculation was used to investigate the reaction mechanisms with seven reaction paths in five different solutions. The values of ΔG were sorted from highest to lowest by levopimaric acid(4), neoabietic acid(3), palustric acid(2), and bietic acid(1). From the perspective of dynamics, the energy barrier in the isomerization of palustric acid(2) to levopimaric acid(4) was the lowest, whereas the highest energy barrier was the isomerization of neoabietic acid(3) to levopimaric acid(4) in the same solution. The addition reaction of levopimaric acid(4) and acrylic acid(5) to acrylopimaric acid c(8) was the optimal reaction path dynamically. However, ΔG of acrylopimaric acid c(8) was higher than that of acrylopimaric acid d(9). In general, the rates of isomerization reactions for rosin resin acids and addition reaction for acrylopimaric acid in water were higher than those in other solvents. HOMO-LUMO and ESP were analyzed for 8 kinds of molecules. For acylpyimaric acid, the non-planar six-memed ring and the C-C double bonds were easily attacked by nucleophile, while the non-planar six-memed ring and the carboxyl group are easily reacted with electrophiles. The highest electrostatic potential of the eight molecules is located at H of the carboxyl group, while the highest electrostatic potential is located at C-O double bond of the carboxyl group.

Keywords: DFT; acrylopimaric acid; reaction mechanisms

1 INTRODUCTION

As a kind of renewable biomass resource, rosin is a crucial forest chemical product[1,2]. However, rosin as a natural resin is used directly, and its additional value needs to be further improved[3]. Rosin resin acids are tricyclic diterpenoid isomers with various components, of which the main component is abietic resin acid[4]. Levopimaric acid(4) with conjugated double bond structure can be formed continuously through the isomerization of abietic acid(1), palustric acid(2), and neoabietic acid(3) under heating condition (Scheme 1)[5]. Levopimaric acid(4) can react with acrylic acid through the Diels–Alder reaction to form isomers of acrylopimaric acid c(8) and acrylopimaric acid d(9) under microwave heat (Scheme 2) [6,7]. As an important modification product of rosin, its additional value is greatly improved. Given that its structure is similar to that of petroleum-based aromatic dicarboxylic acids, such as isophthalic acid and terephthalic acid, acrylopimaric acid is considered one of the possible substitutes for petroleum-based polymeric monomers[8,9]. The modification and application of acrylopimaric acid have been reported in the literature[10]. For example, acrylopimaric acid is prepared into surfactants, UV-curable coatings, polyurethane, epoxy resin, and polyester[11,12]. However, the mechanisms underlying the isomerization of levopimaric acid and the Diels–Alder addition reaction of acrylpimaric acid have not been studied in detail.

Quantum chemistry is one of the most reliable methods to study the mechanism of microscopic reactions[13]. Quantum chemistry theory, density functional theory (DFT), and molecular dynamics play an important role in the study of organic reactions[14]. DFT has become a reliable and powerful tool for studying the kinetics, byproduct formation, and mechanism of organic reactions at the molecular level[15-18]. DFT was used to investigate the formation of acrylopimaric acid, and the effects of different solutions on the reaction were discussed. The isomerization of the four resin acids and the addition mechanism of acrylopimaric acid should be revealed to provide a theoretical basis for the large-scale synthesis of acrylopimaric acid, the selection of appropriate solvents, and the optimization of related process parameters.

2 EXPERIMENTAL

2.1 DFT calculations

Theoretical calculation was performed using Gaussian 09 software[19]. Geometric optimization of the reactants, products, and transition state (TS) [20] structures was performed at the M062X/ 6-31G (d) level using the SMD[21] solvent model, and the temperature was set at 453 K. All reactants and products had no imaginary frequency, and the TS had only one virtual frequency. Intrinsic reaction coordinate analysis was performed at the same level to verify the relationship among reactants, TSs, and products[22]. M062X/def2TZVP was used to calculate the single point energy and obtain more precise results with the SMD solvent model. Gibbs free energies were corrected[23,24].

According to the thermodynamic formula of TS theory (TST), the rate constant k^{TST} is calculated as follows[25,26]:

$$k^{TST} = \sigma \frac{k_B T}{h} \left(\frac{RT}{P_0}\right)^{\Delta n} e^{\frac{-G^{\neq}(T)}{k_B T}} \quad (1)$$

$$\sigma = \frac{\sigma_{rot,R}}{\sigma_{rot,TS}} \quad (2)$$

$$G^{\neq}(T) = G_{TS}(T) - G_R(T) \quad (3)$$

$\sigma_{rot,R}$ and $\sigma_{rot,TS}$ are rotational symmetry of the reactants and TSs. h is Planck's constant, σ and k_B are the degeneracy of reaction and Boltzmann's constant, respectively. $G^{\neq}(T)$ represents the standard Gibbs free energy of activation for the considered reaction and Δn=n-1 for bimolecular or unimolecular reactions.

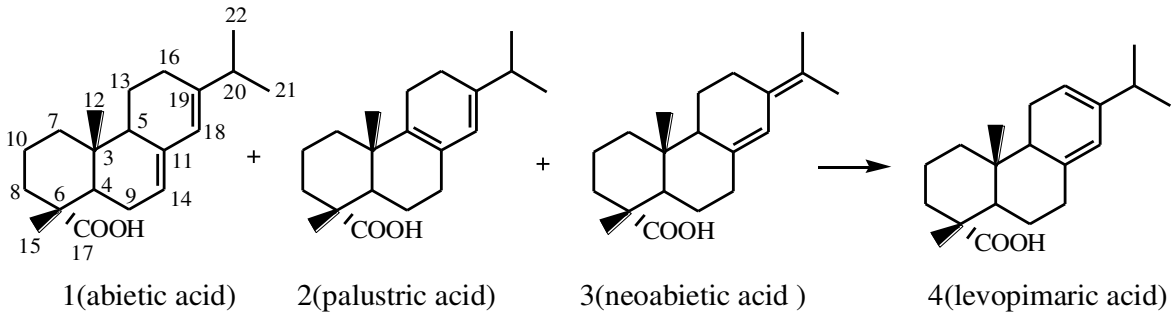

Scheme 1. Four Abietic Resin Acids

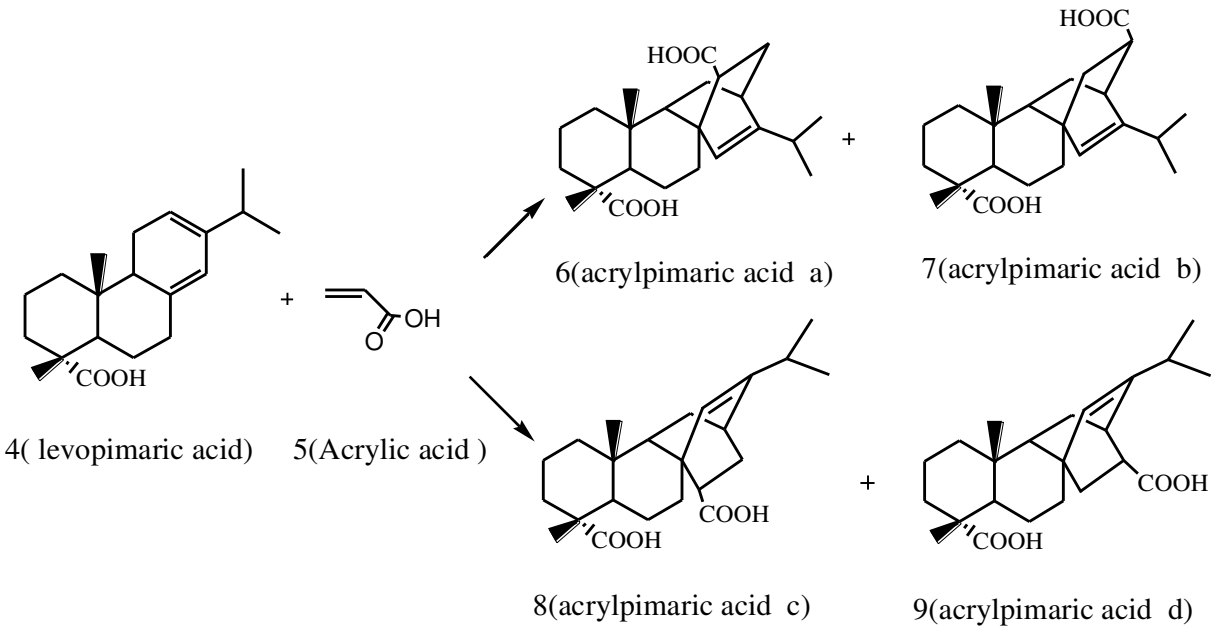

Scheme 2. Levopimaric Acid Reacts with the addition of Acrylic Acid

3 RESULTS AND DISCUSSION

3.1 Reaction mechanism and reaction paths

The mechanism underlying the isomerization of acid resins is shown in Scheme 3, and the reaction of levopimaric acid with the addition of acrylic acid via four reaction paths is shown in Scheme 4. In all reactions, the structures of stationary points are shown in Fig. 1-3. H on C16 migrated to C18. Subsequently, H on C18 migrated to C14. The double bonds of C18-C19 and C11-C14 became single bonds, and the conjugated double bonds formed C16-C19 and C11-C18. Abietic acid(1) isomerized to levopimaric acid(4). During this process, the energy barrier of TS142 determined the reaction rate with increasing energy. H on C16 migrated to C5. The double bonds of C5-C11 and C18-C19 became single bonds, and the conjugated double bonds formed C16-C19 and C11-C18. Palustric acid(2) isomerized to levopimaric acid(4). H on C16 migrated to C20. Neoabietic acid(3) isomerized to levopimaric acid(4).

The C-C double bond of acrylic acid(5) gradually approached the C18-C19 single bond of levopimaric acid(4), and the six-membered ring of the conjugated double bond of levopimaric acid(4) became non-coplanar, forming a boat structure. The double bond between C18 and C19 became a single bond, and H was not migrated during this

process. As a result of the different locations of the addition reaction between levopimaric acid(4) and acrylic acid(5), four different reaction paths were noted, and acrylopimaric acid with different structures formed.

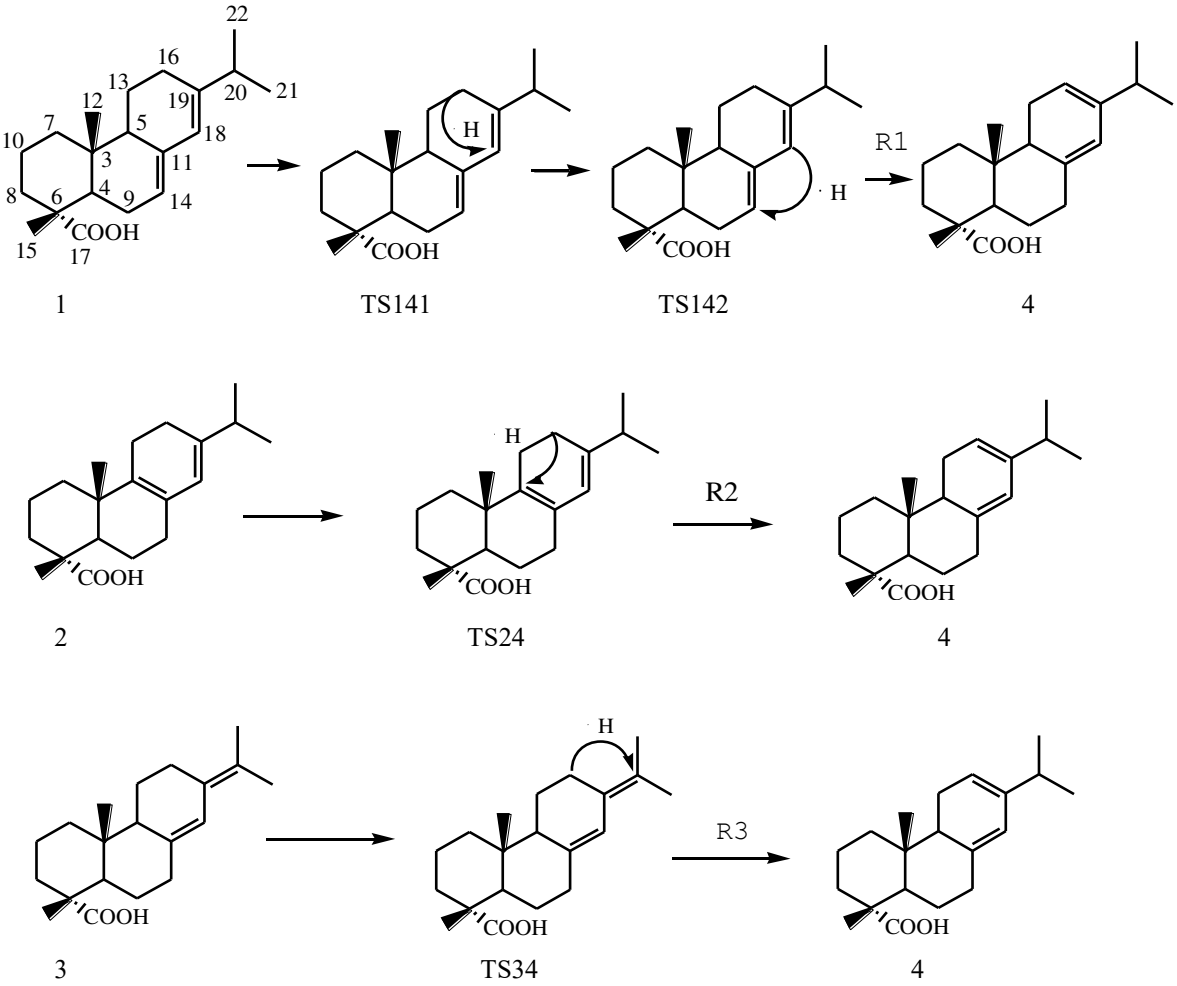

Scheme 3. Mechanism of Isomerization about Acid Resins

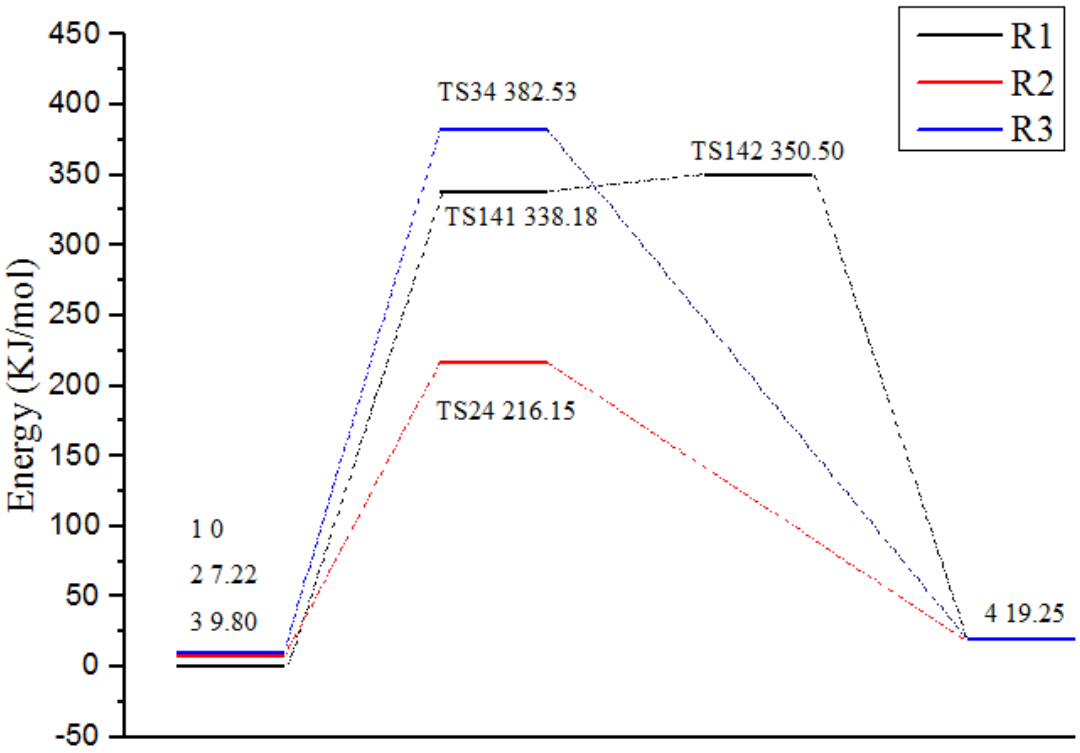

Figure 1. Energy diagram of R1-3

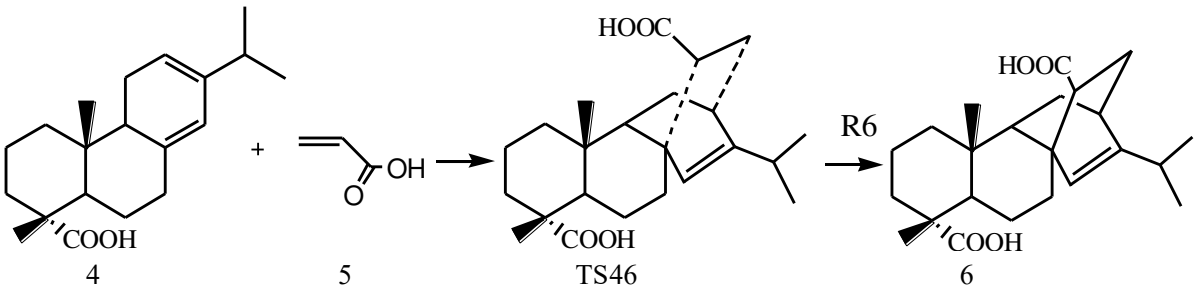

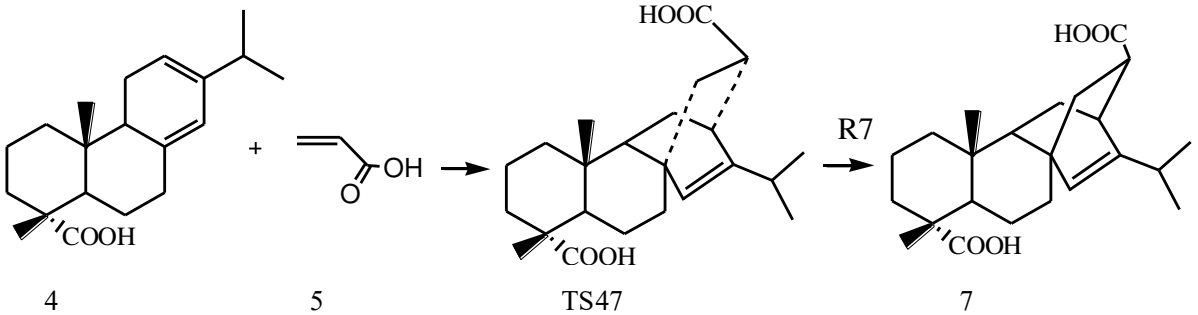

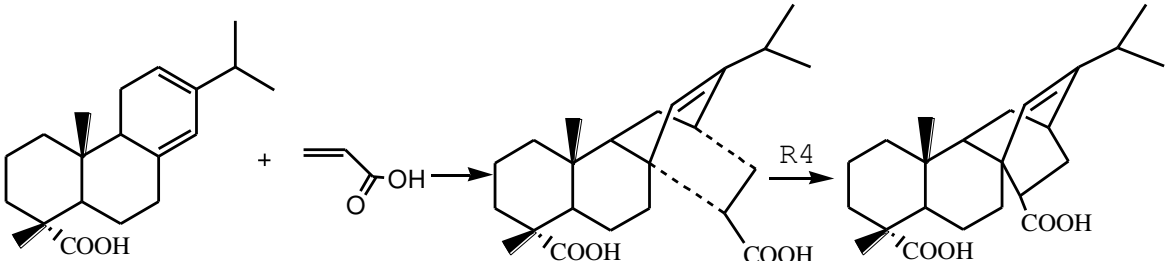

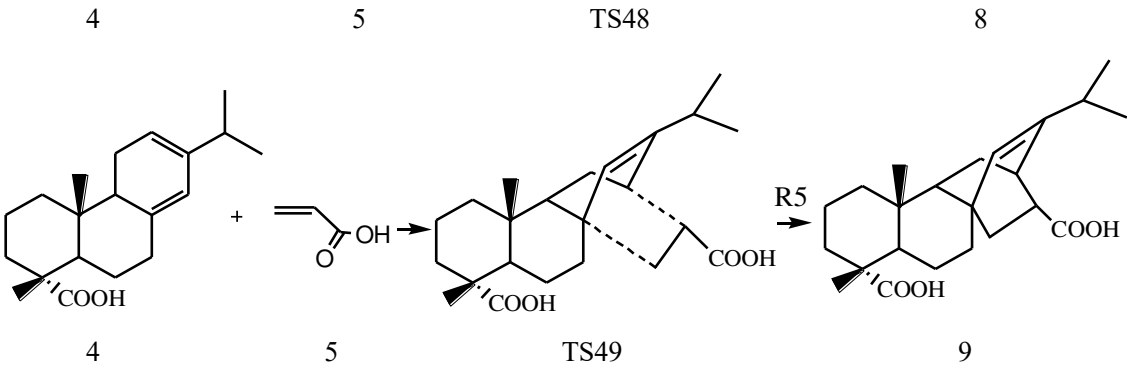

Scheme 4. Four Reaction Paths Involved in the Reaction of Levopimaric Acid with the addition of Acrylic Acid

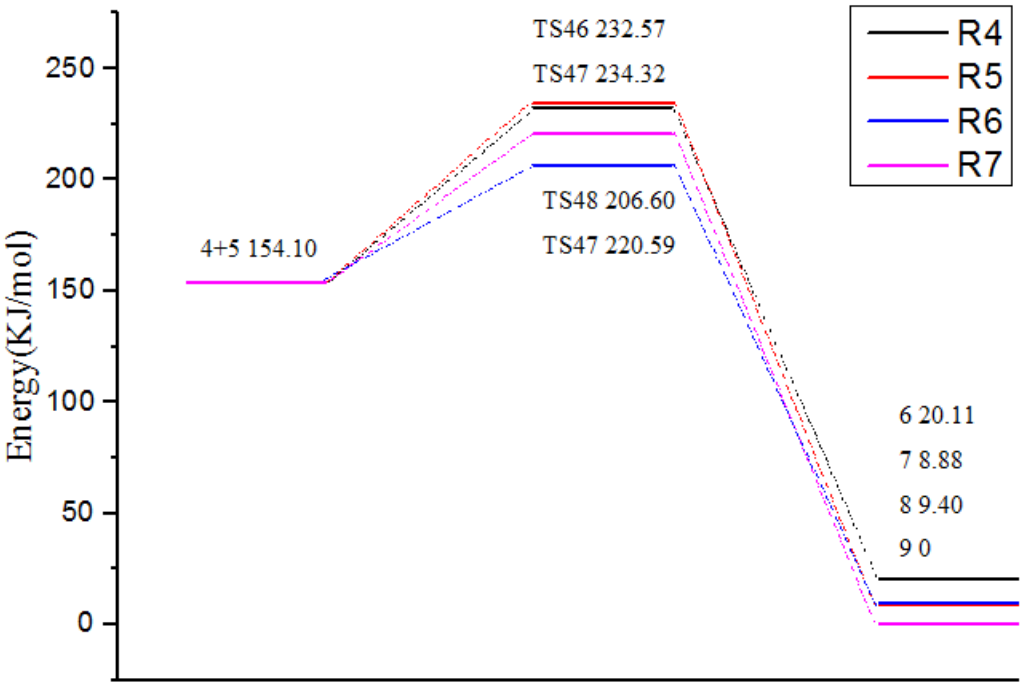

Figure 2. Energy diagram of R4-6

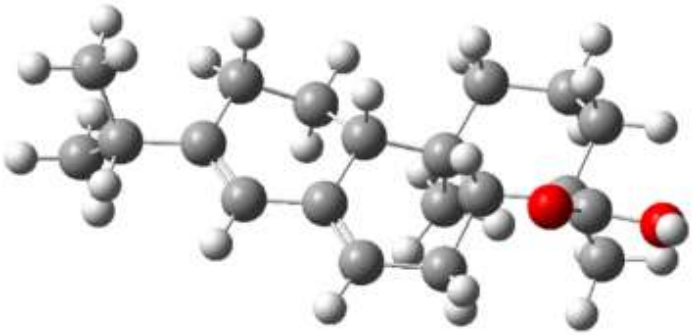

1

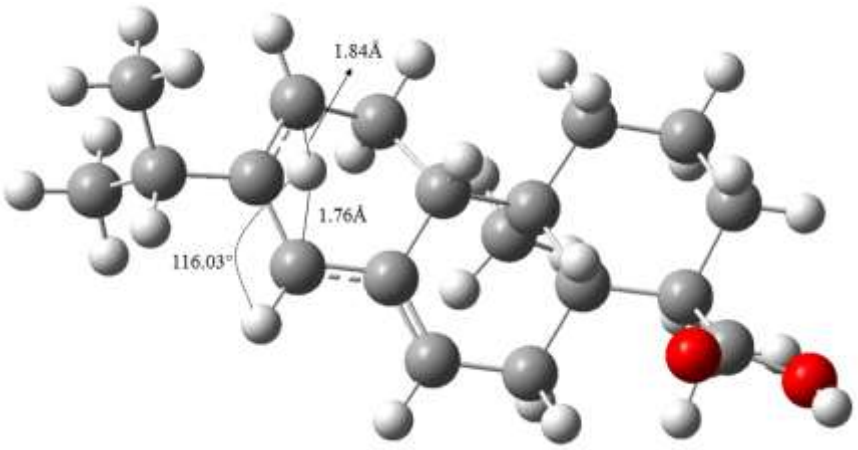

TS141

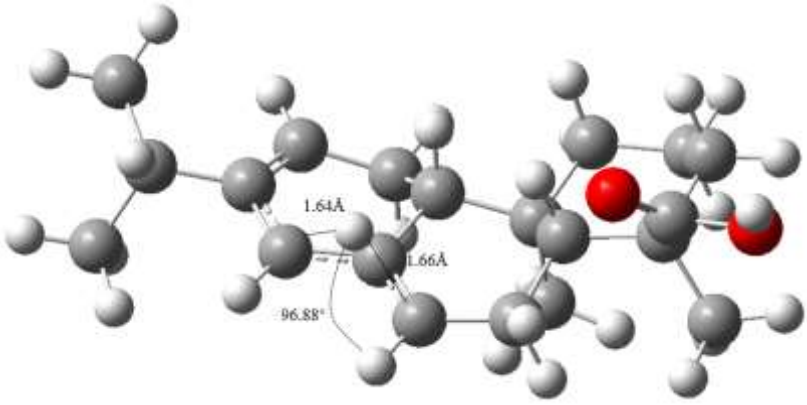

TS142

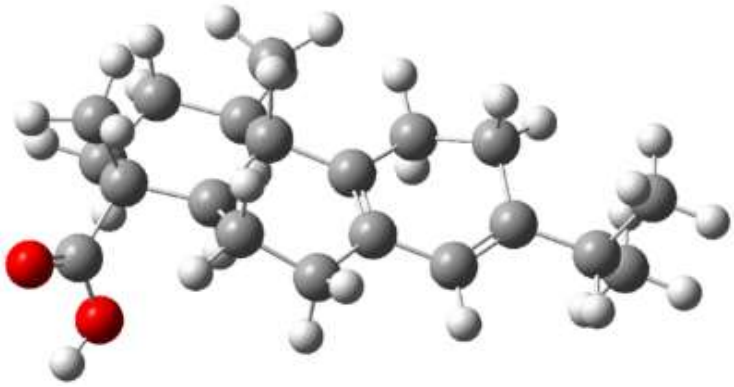

2

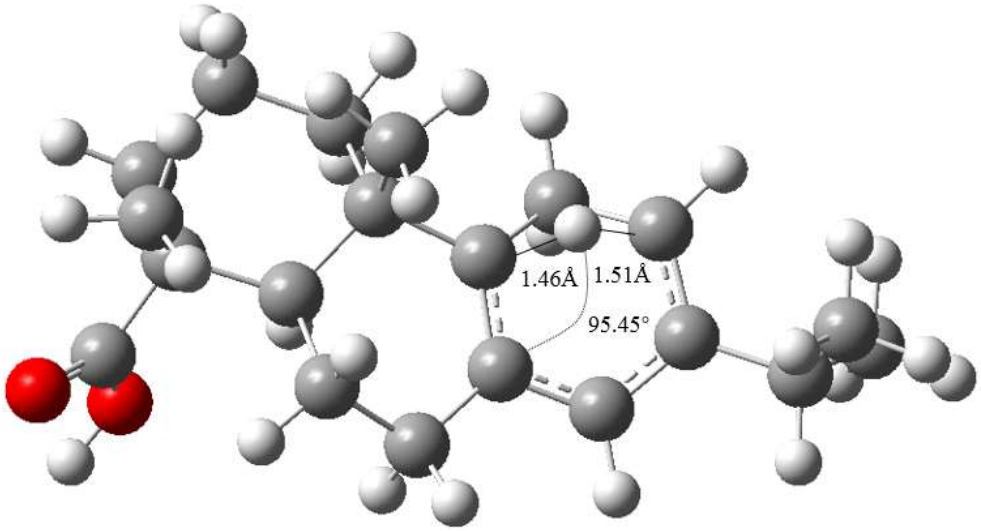

TS24

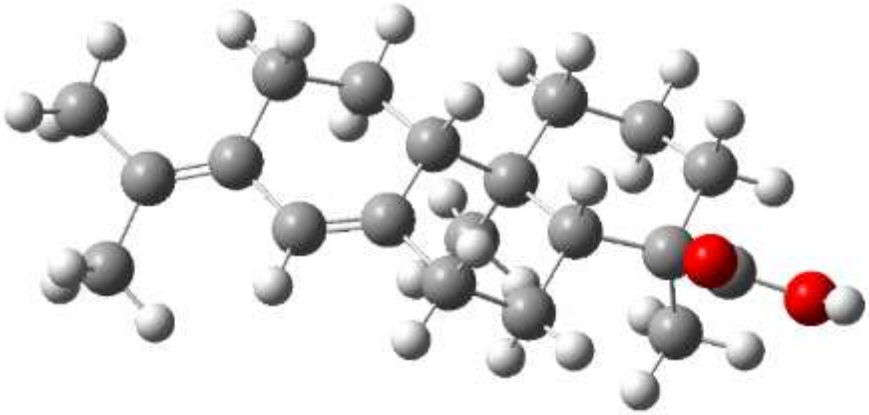

3

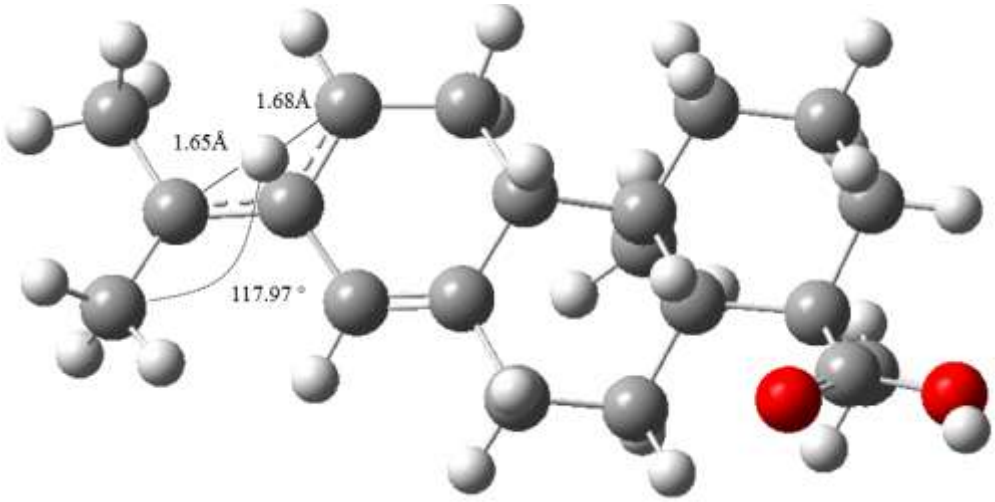

TS34

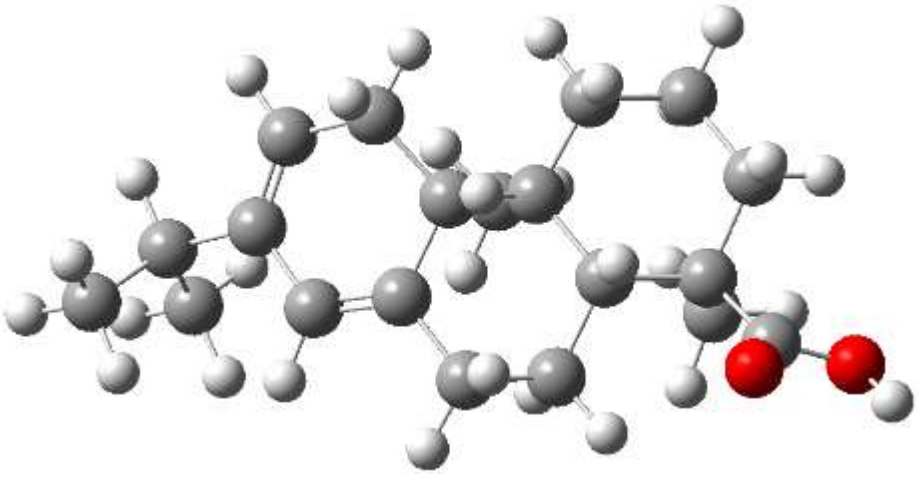

4

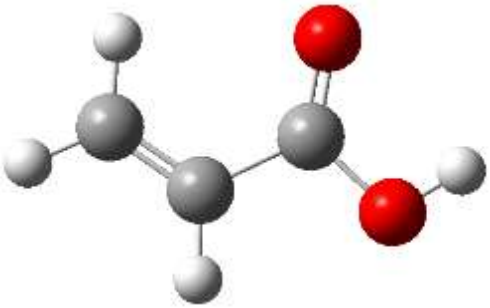

5

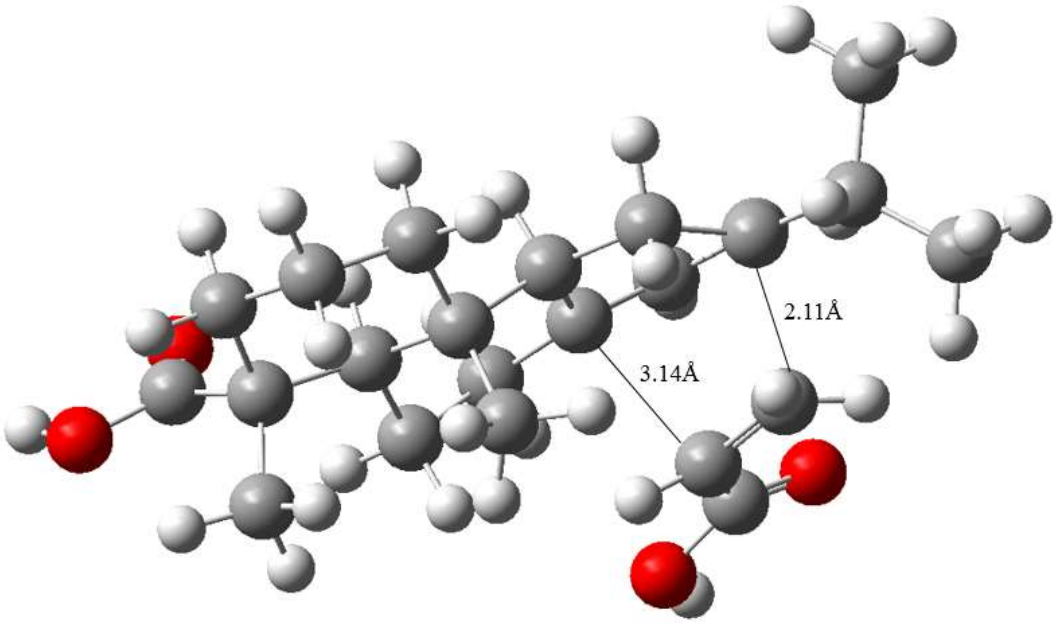

TS46

6

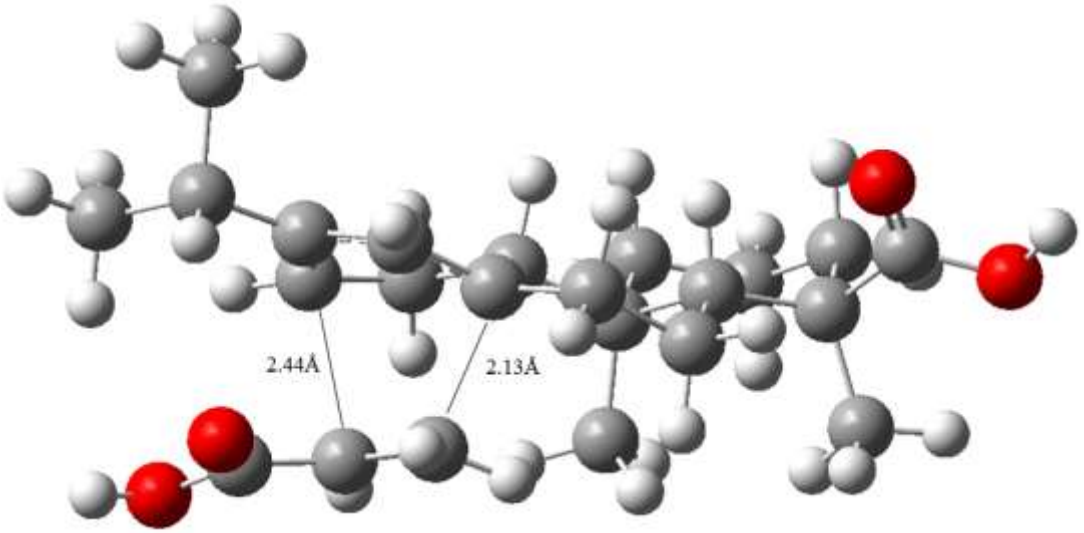

TS47

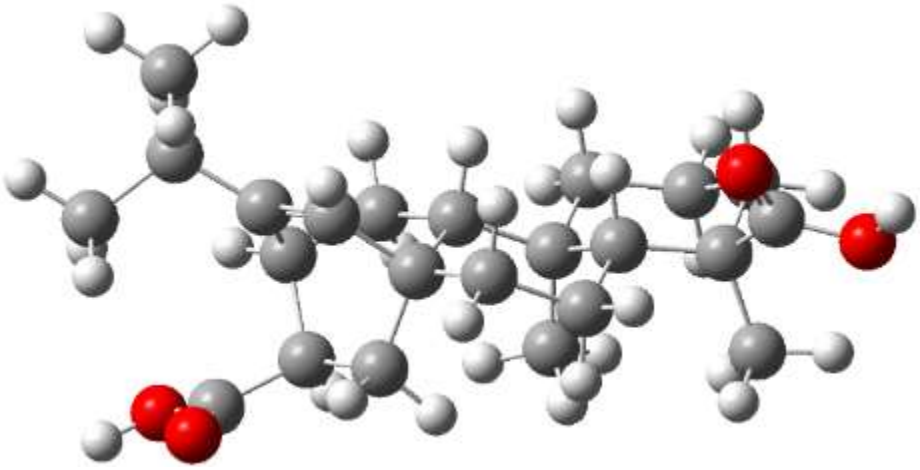

7

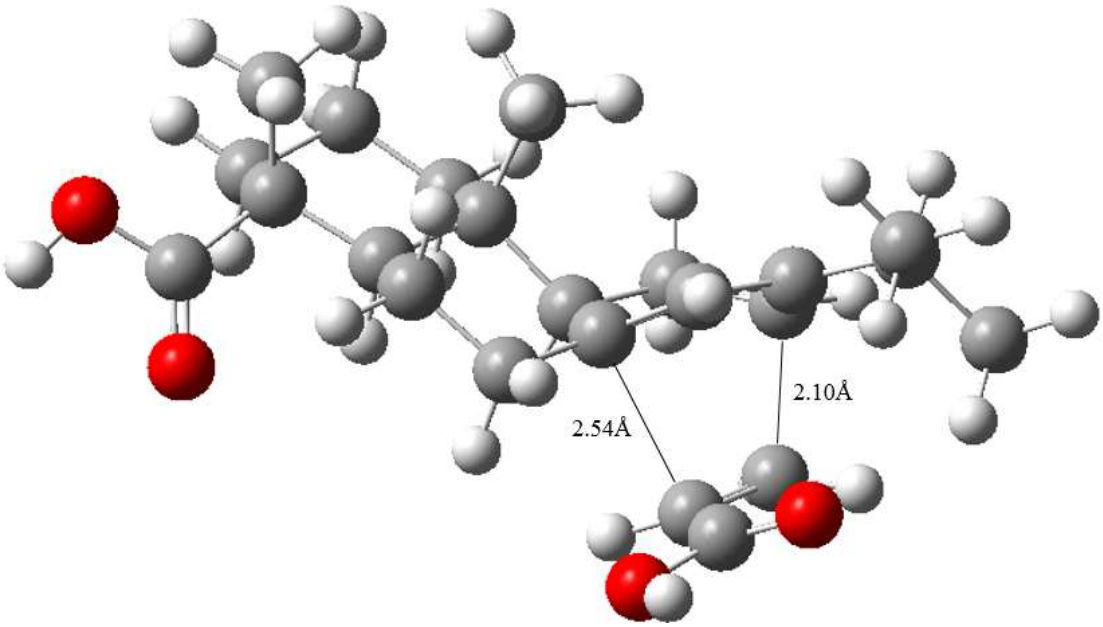

TS48

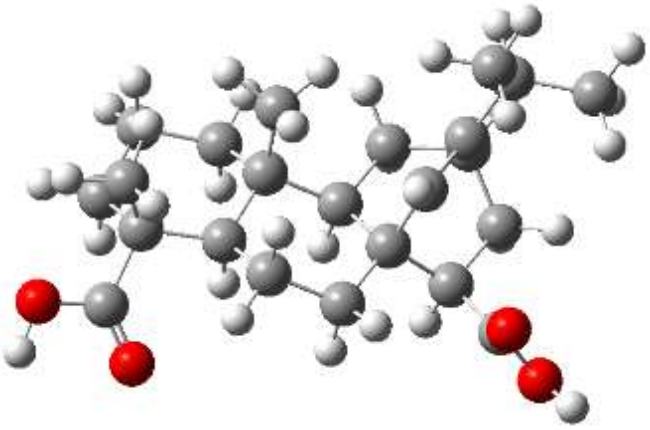

8

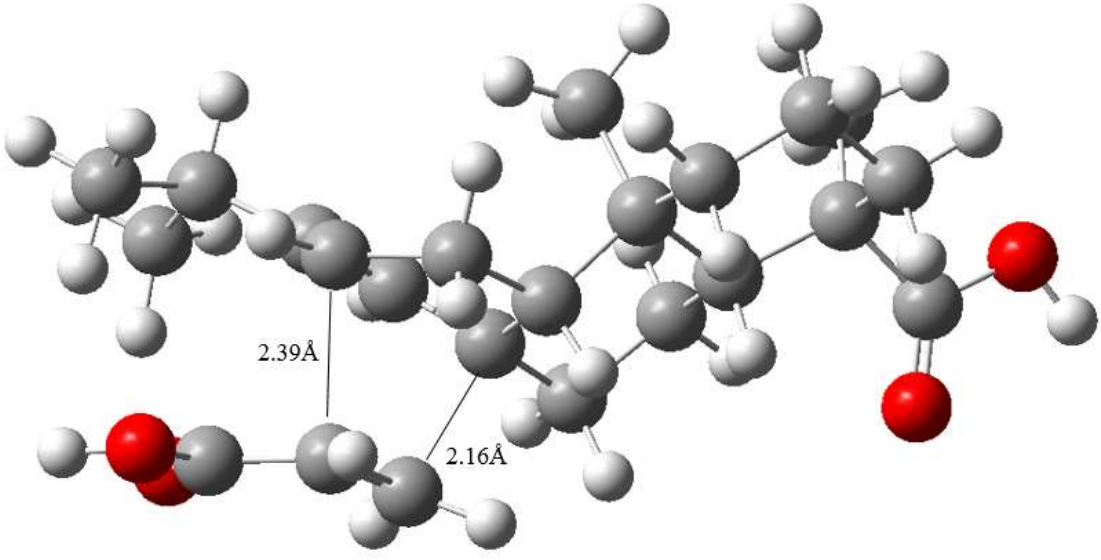

TS49

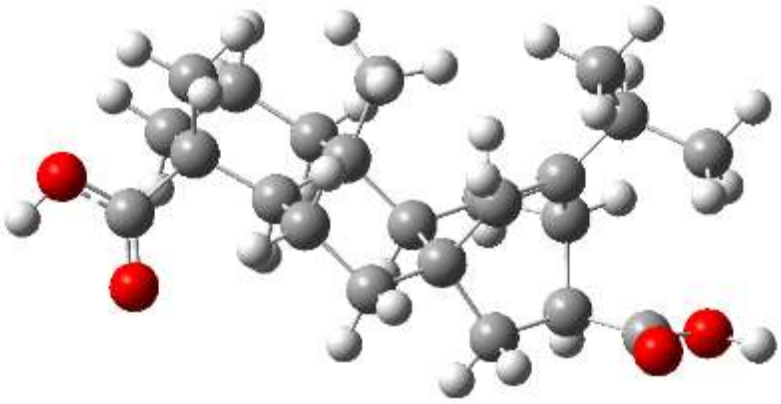

9

Figure 3. Structures of stationary Points

3.2 Thermodynamics and kinetics of reactions in different solvents

From the perspective of thermodynamics, the isomerizations of bietic acid(1), palustric acid(2), and neoabietic acid(3) into levopimaric acid(4) exhibited an exothermic reaction (Table 1). The values of ΔG were sorted from highest to lowest by levopimaric acid(4), neoabietic acid(3), palustric acid(2), and bietic acid(1). ΔG of levopimaric acid(4) was 19.25 KJ/mol in the solvent-free reaction and 18.22 KJ/mol in acetic acid, which was higher than the value of bietic acid(1). From the perspective of dynamics, the energy barrier in the isomerization of palustric acid(2) to levopimaric acid(4) was the lowest, whereas the highest energy barrier was the isomerization of neoabietic acid(3) to levopimaric acid(4) in the same solution. In aqueous solution, the lowest energy barrier in the isomerization of bietic acid(1) to levopimaric acid(4) was 342.36 KJ/mol, and the lowest energy barrier in the isomerization of neoabietic acid(3) to levopimaric acid(4) was 369.50 KJ/mol. In DMSO solution, the lowest energy barrier in the isomerization of palustric acid(2) to levopimaric acid(4) was 209.28 KJ/mol. However, the energy barriers in the isomerization of the three resin acids to levopimaric acid(4) increased in varying degrees in DMF solution and acetic acid solution. The high energy barrier of the isomerization of the three resin acids into levopimaric acid(4) indicates that the hydrogen transfer in the reaction is harsh. In the experiment, the reactants are usually heated by microwave to a high temperature of 453-523 K, with long reaction time of 1.5-10 h. The calculation is verified with the experimental results[6].

From the perspective of thermodynamics, the Diels–Alder addition reaction of levopimaric acid(4) and acrylic acid(5) to acrylopimaric acid was exothermic (Table 2). The ΔG value of acrylopimaric acid d(9) was the lowest, and the addition reaction of levopimaric acid(4) and acrylic acid(5) to acrylopimaric acid d(9) was the optimal reaction path thermodynamically. However, from the perspective of dynamics, the energy barrier in the addition reaction of levopimaric acid(4) and acrylic acid(5) to acrylopimaric acid c(8) was the lowest (Table 3). The energy barrier of TS49 in the process of generating acrylopimaric acid d(9) was 13.99 KJ/mol higher than that of TS48, which was lower than that of TS46 and TS47. The addition reaction of levopimaric acid(4) and acrylic acid(5) to acrylopimaric acid c(8) was the optimal reaction path dynamically. The energy barriers generated by the addition of levopimaric acid(4) and acrylic acid(5) to acrylopimaric acid c(8) or acrylopimaric acid d(9) in aqueous solution were lower than those of other solvents.

The reaction rates k of isomerizations in order from fast to slow were palustric acid(2), abietic acid(1), and neoabietic acid(3) as shown in Table 4. The reaction rates k of the isomerizations of abietic acid(1) and neoabietic acid(3) in aqueous solution were faster than those of other solvents. However, the reaction rate k of the isomerization of palustric acid(2) to levopimaric acid(4) in DMSO solution was faster than that of other solvents. The reaction rates k of the addition reaction of levopimaric acid(4) and acrylic acid(5) to acrylopimaric acid in aqueous solution

were faster than those of other solvents. However, the reaction rates k were lower in varying degrees in DMF solution and acetic acid solution. Therefore, water is a better solvent for the reactions than the other solvents.

Table 1 Energy of the isomerization of abietic acid resins in different solutions

solvent / ΔG(KJ/mol)	solvent-free	water	DMSO	DMF	acetic acid
1	0	0	0	0	0
2	7.22	7.07	6.34	5.61	5.28
3	9.80	11.16	11.17	10.45	9.91
4	19.25	19.39	19.89	18.95	18.22
TS141	338.18	335.32	332.75	308.61	316.48
TS142	350.50	342.36	342.62	377.08	379.21
TS24	216.15	216.17	215.62	222.98	222.98
TS34	382.53	380.66	380.87	414.87	416.11

Table 2 Energy of the reaction of levopimaric acid with acrylic acid in different solutions

solvent / ΔG(KJ/mol)	solvent-free	water	DMSO	DMF	acetic acid
4+5	154.10	156.74	148.38	134.88	151.36
6	20.11	18.33	18.35	19.26	20.46
7	8.88	8.13	7.80	7.96	8.93
8	9.40	8.83	8.76	9.89	10.52
9	0	0	0	0	0
TS46	232.57	225.21	232.75	233.74	227.68
TS47	234.32	225.10	231.47	234.70	230.57
TS48	206.60	198.53	206.88	206.68	200.73
TS49	220.59	213.76	219.79	222.74	218.78

Table 3 Activation energy Ea in the isomerization of abietic resin acids and addition of levopimaric acid with acrylic acid

solvent / Ea(KJ/mol)	solvent-free	water	DMSO	DMF	acetic acid
1 → 4	350.50	342.36	342.62	377.08	379.21
2 → 4	208.93	209.1	209.28	217.37	217.7
3 → 4	372.73	369.5	369.70	404.87	406.2
4+5 → 6	78.47	68.47	84.37	98.86	76.32
4+5 → 7	80.22	68.36	83.09	99.82	79.21
4+5 → 8	52.50	47.79	58.50	71.8	49.37
4+5 → 9	66.49	57.02	71.41	87.86	67.42

Table 4 Reaction Rates k in the Isomerization of Abietic resin acids and addition of Levopimaric Acid with Acrylic Acid

solvent / $k(s^{-1})$	solvent-free	water	DMSO	DMF	acetic acid
1 → 4	$1.87x10^{-28}$	$1.63x10^{-27}$	$1.52x10^{-27}$	$1.61x10^{-31}$	$9.16x10^{-32}$
2 → 4	$3.95x10^{-12}$	$3.77x10^{-12}$	$3.60x10^{-12}$	$4.20x10^{-13}$	$3.84x10^{-13}$
3 → 4	$5.12x10^{-31}$	$1.21x10^{-30}$	$1.14x10^{-30}$	$1.01x10^{-34}$	$7.07x10^{-35}$
4+5 → 6	$4.35x10^{3}$	$6.19x10^{4}$	$9.09x10^{2}$	$1.94x10^{1}$	$7.70x10^{3}$
4+5 → 7	$2.74x10^{3}$	$6.38x10^{4}$	$1.28x10^{3}$	$1.50x10^{1}$	$1.72x10^{2}$
4+5 → 8	$4.30x10^{6}$	$1.50x10^{7}$	$8.74x10^{5}$	$2.56x10^{4}$	$9.87x10^{6}$
4+5 → 9	$1.05x10^{5}$	$1.30x10^{6}$	$2.60x10^{4}$	$3.60x10^{2}$	$8.18x10^{4}$

3.3 HOMO–LUMO analysis

The energies of HOMO and LUMO are calculated to obtain an overall description of the reaction[27,28]. The gap between HOMO and LUMO is determined by the chemical reactivity, kinetic stability, and electronic properties of the molecule[29]. The HOMO of the molecule has a relatively loose bond to its electrons and has an electron donor property, whereas the LUMO has a strong affinity for electrons and has an electron acceptor property. I ($-E_{HOMO}$) and A ($-E_{LUMO}$) are the vertical ionization energy and vertical electron affinity, respectively. The chemical potential and global hardness are concepts of molecular structure stability and reactivity that are calculated using the equations $\mu = -(I + A)/2$ and $\eta = (I - A)/2$. ω is the electrophilicity index that is calculated using the equation $\omega = \mu^2/2\eta$. B3LYP-D3(BJ)/6-311G* is calculated about HOMO–LUMO gaps. The lower hardness, chemical potential and energy gap facilitate charge transfer and indicates enhancement in the species, reactivity.

As shown in figure 4, the active sites of the four isomeric resin acids were the C-C double bonds where the six-member ring is located, and both C-C double bonds are easily attacked by both electrophiles and nucleophiles. For acylpyimaric acid, the non-planar six-memed ring (C53 and C55) and the C-C double bonds were easily attacked by nucleophile, while the non-planar six-memed ring (C9 and C15) and the carboxyl group (O1 and O2) are easily reacted with electrophiles. Given the similar structure of isomers, the greater the gap of HOMO–LUMO, the higher the chemical stability of the molecule. The gap of abietic acid(1) was 0.2111 eV higher than that of palustric acid(2), whereas the gap was 0.1859 eV higher than that of neoabietic acid(3) (Table 5). Combined with the previous calculation of TS, neoabietic acid(3) was the easiest to be isomerized into levopimaric acid(4), followed by palustric acid(2); the isomerization rate of abietic acid(1) was the slowest. The gap of HOMO–LUMO and TS of acrylopimaric acid reveled that acrylopimaric acid c(8) was the most easily formed by the addition reaction of levopimaric acid(4) and acrylic acid(5). Combined with the previous calculation of TS, the gap had a certain positive correlation with potential barrier, which verified the correctness of the calculated results. The higher electrophilicity index of levopimaric acid(4), it is more likely to partially interact with molecular electronegativity. HOMO and LUMO orbitals of four resin acids overlap, and the two conjugated C=C double bonds of six-membered rings are the main active sites, which can undergo isomerization and addition reactions. Due to the presence of isopropyl substituents at the reaction site of levopimaric acid, the addition product propimaric acid has two structural isomers, affected by the steric hindrance of the six-member ring of the product. Levopimaric acid(4) is dienes, and two C=C conjugated double bonds of the six-membered ring are HOMO orbital regions with electron-donor properties. Acrylic acid(5) is the dienophile, and its C=C double bond is in the LUMO orbital region with electron-philic. Orbitals have electron donor properties. This is conducive for Diels-Alder reaction.

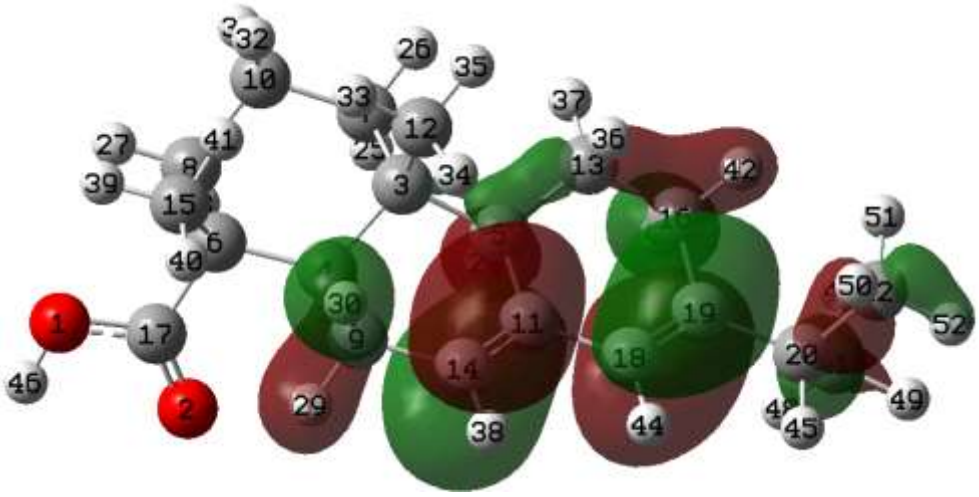

1 HOMO

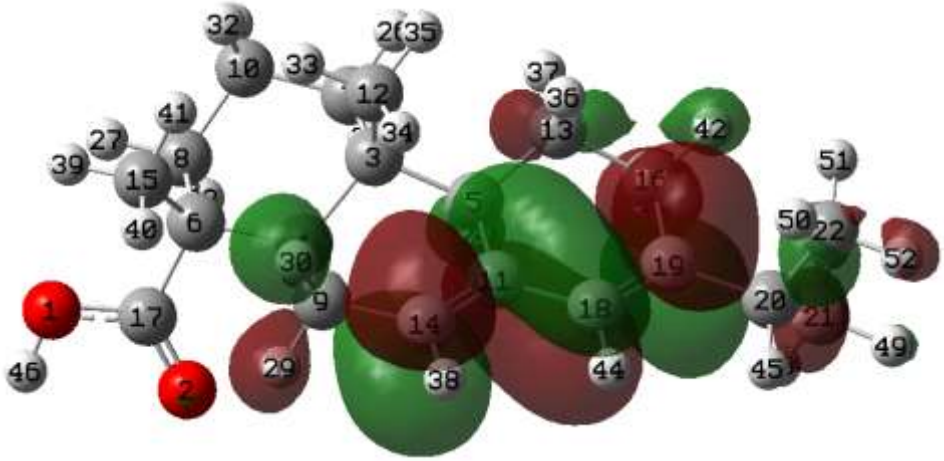

1 LUMO

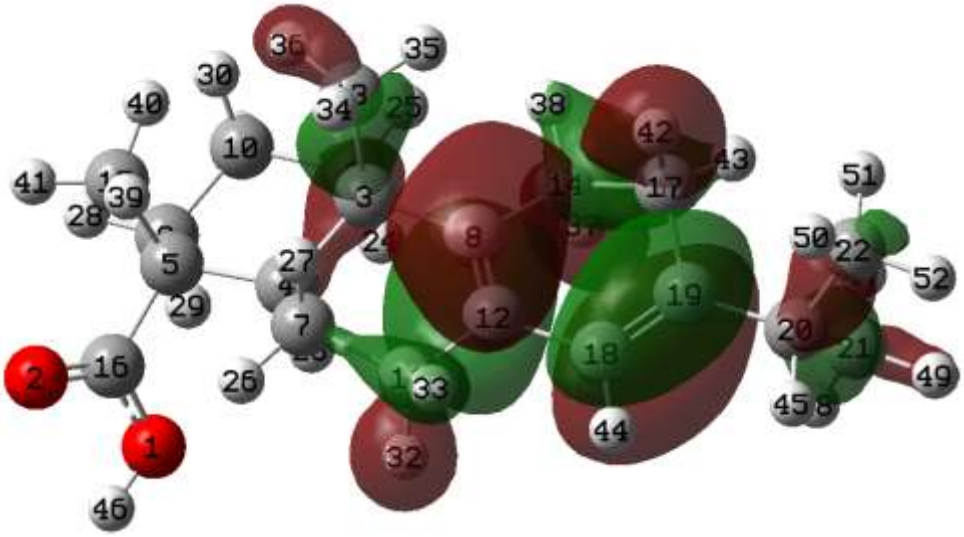

2 HOMO

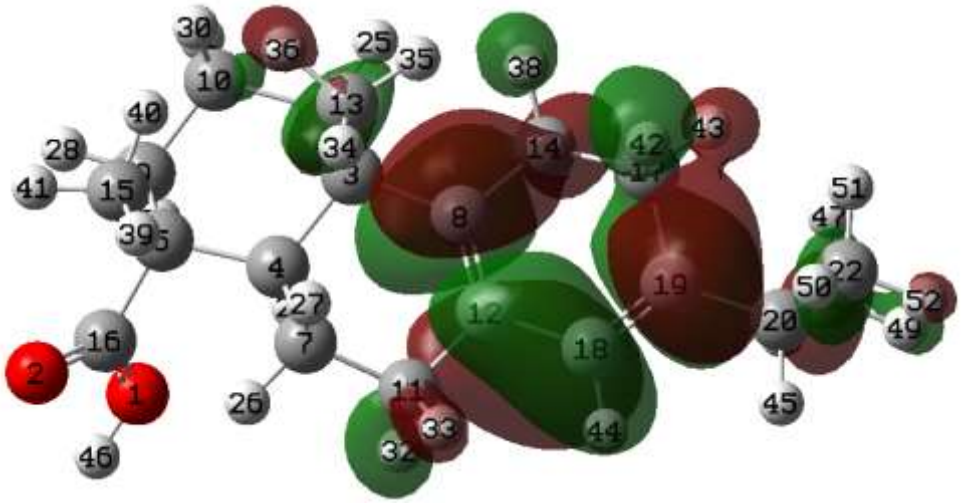

2 LUMO

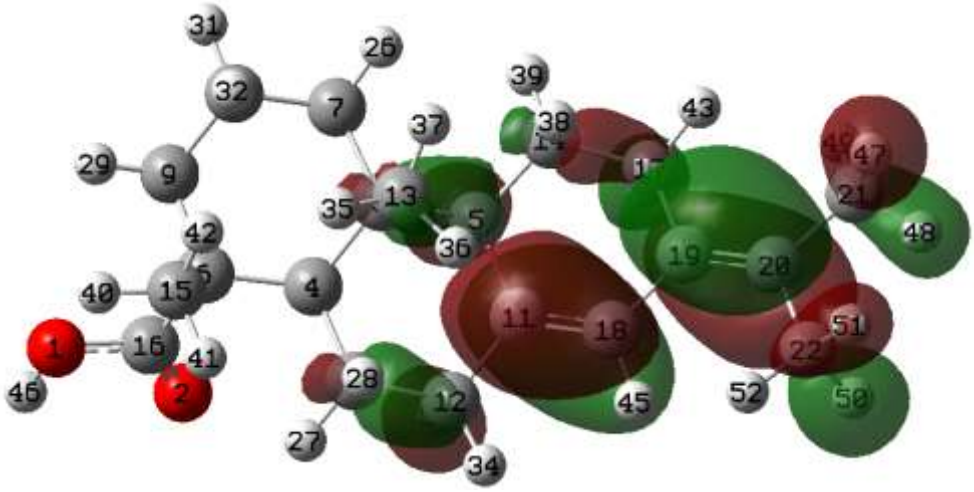

3 HOMO

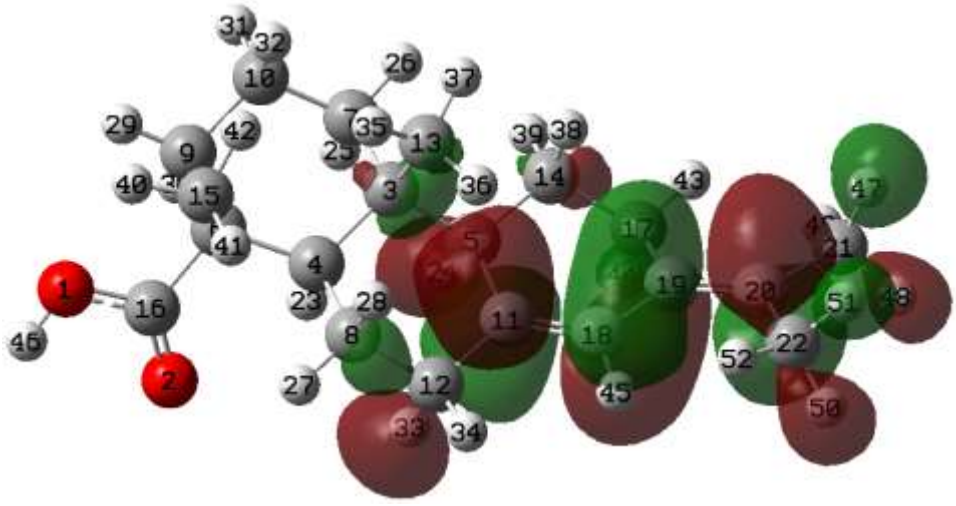

3 LUMO

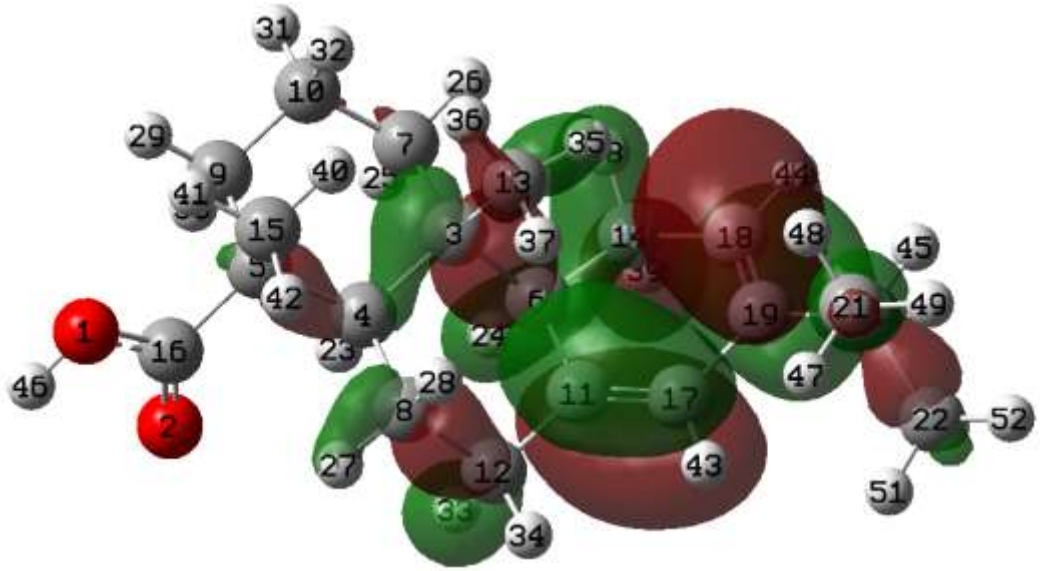

4 HOMO

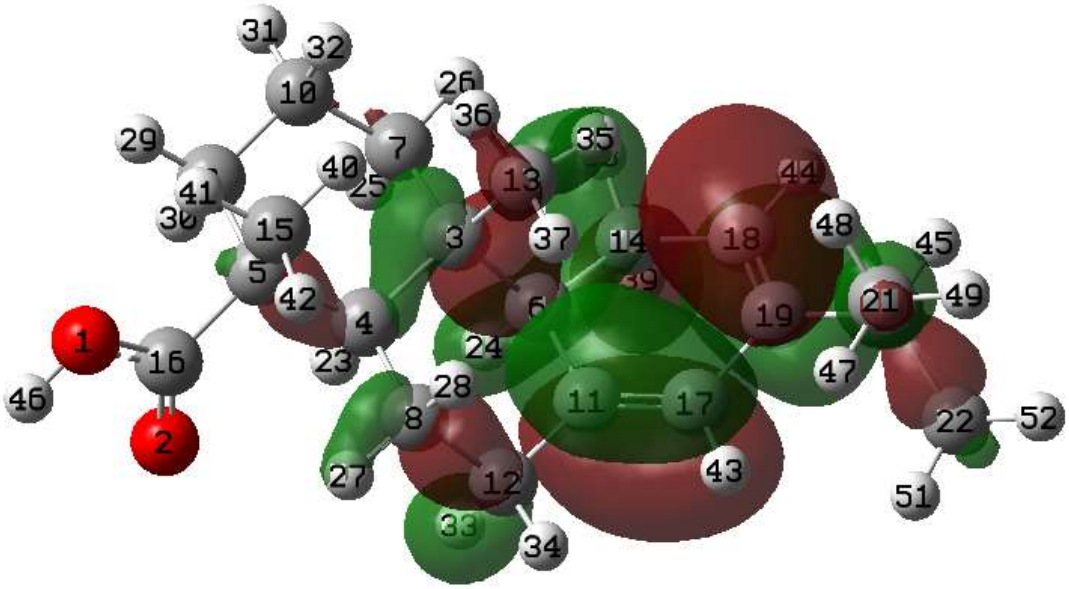

4 LUMO

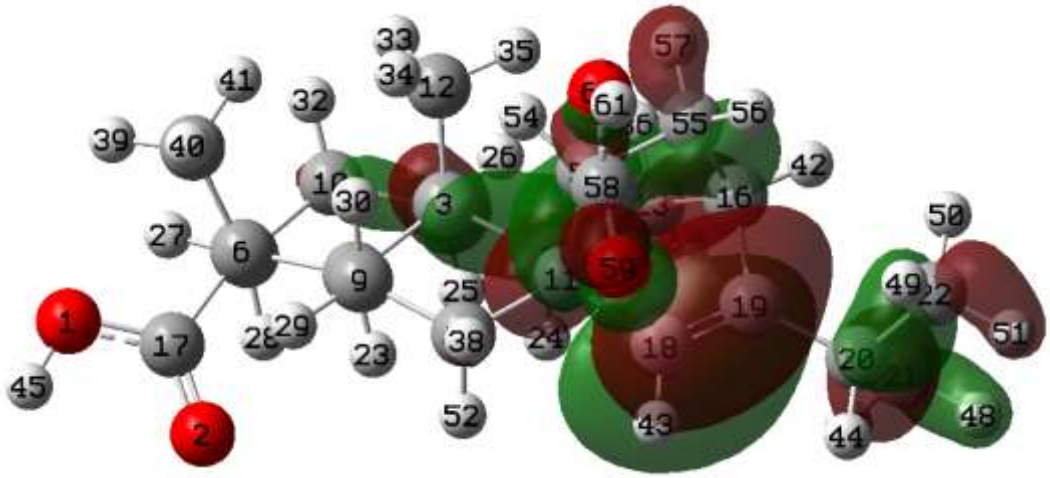

6 HOMO

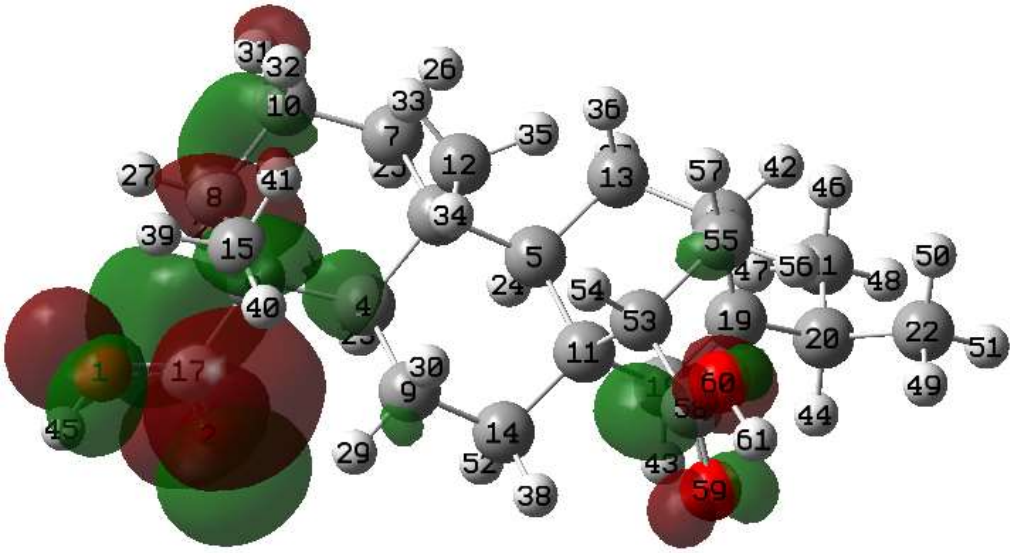

6 LUMO

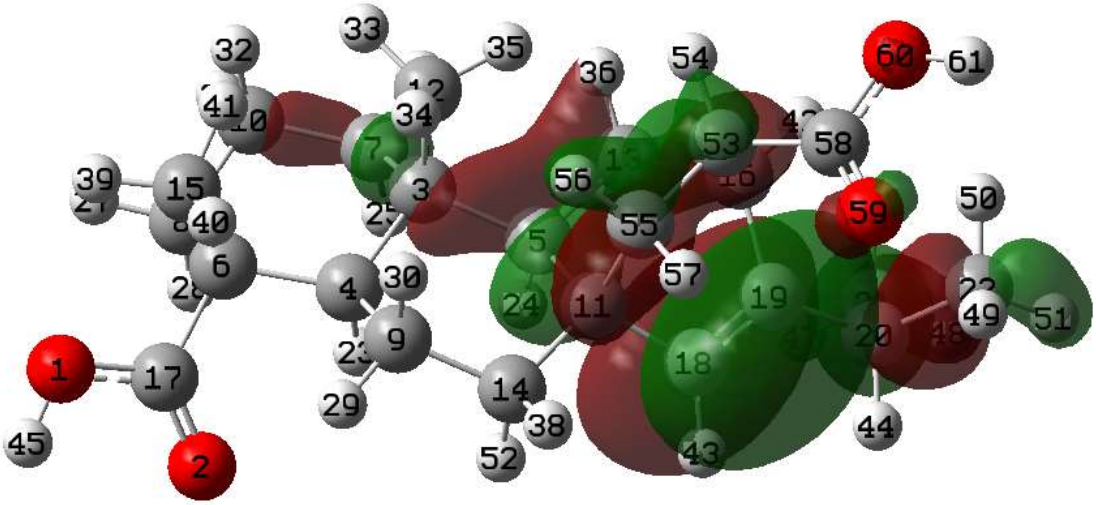

7 HOMO

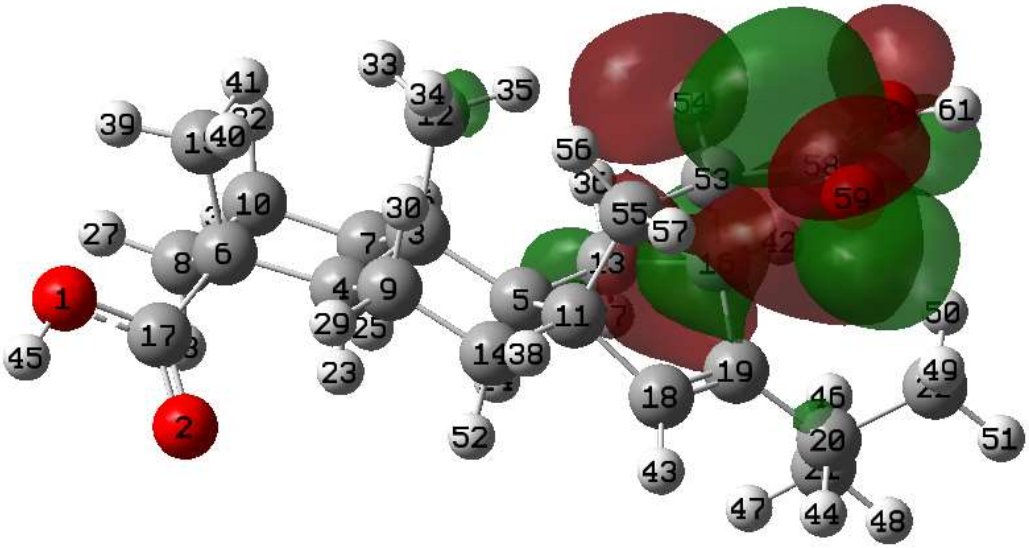

7 LUMO

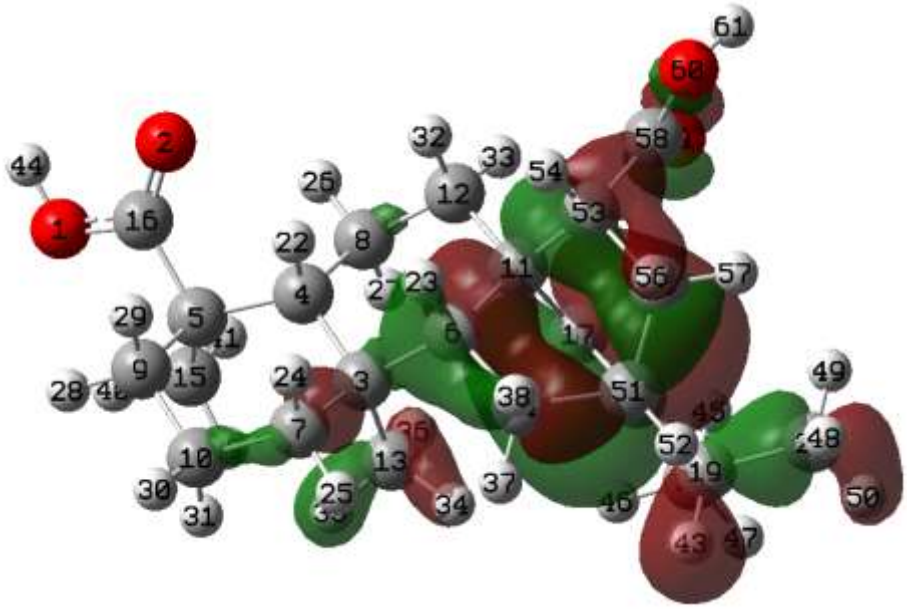

8 HOMO

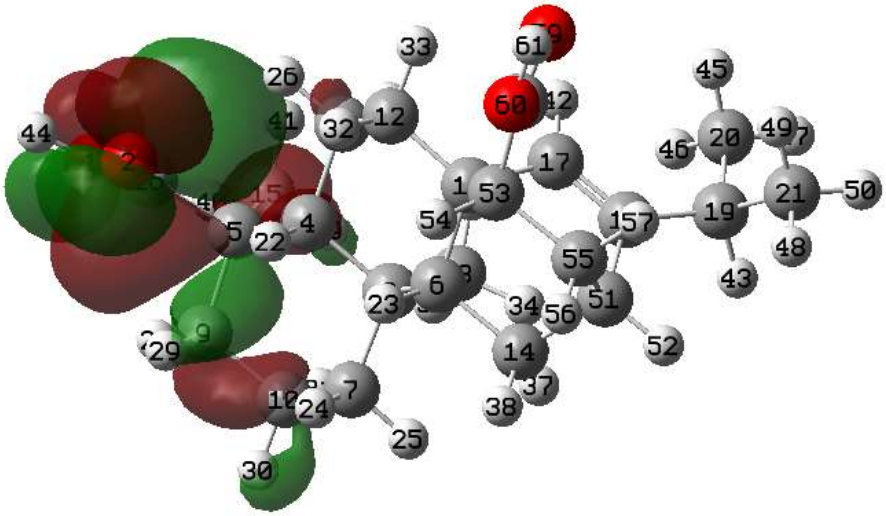

8 LUMO

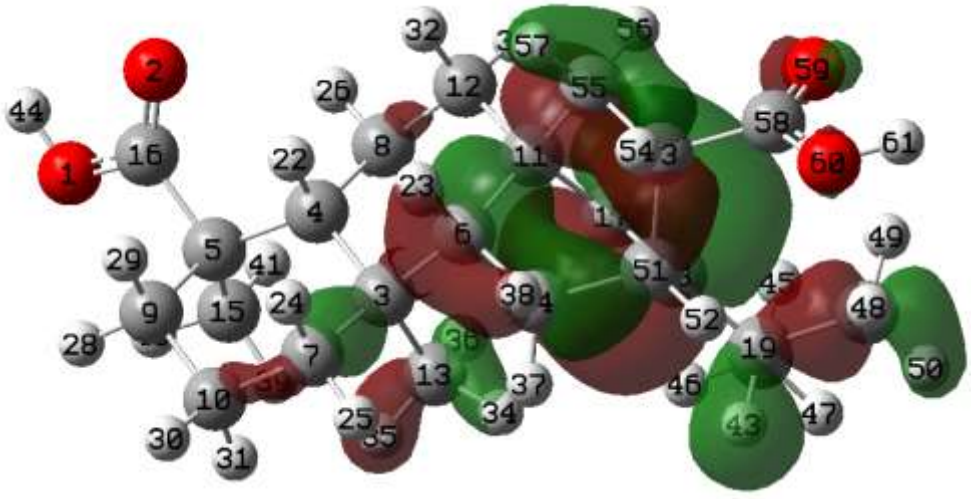

9 HOMO

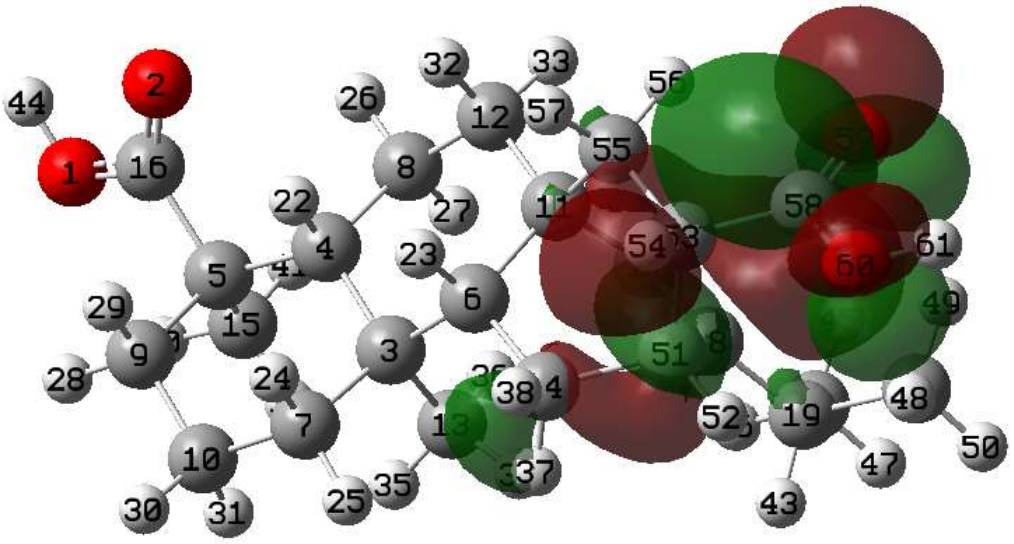

9 LUMO

Figure 4. Frontier molecular orbitals of HOMO and LUMO

Table 5 Quantum Molecular Descriptors (eV) for optimized Geometries

Species	HOMO	LUMO	Gap	I	A	μ	η	ω
1	-6.7408	0.9090	7.6498	6.7408	-0.9090	-2.9159	3.8249	1.1115
2	-6.6524	0.7860	7.4384	6.6524	-0.7860	-2.9332	3.7192	1.1567
3	-6.6155	0.8484	7.4639	6.6155	-0.8484	-2.8836	3.7320	1.1140
4	-6.6304	0.6340	7.2644	6.6304	-0.6340	-2.9982	3.6322	1.2374
6	-7.5576	1.6462	9.2038	7.5576	-1.6462	-2.9557	4.6019	0.9492
7	-7.6936	1.5541	9.2477	7.6936	-1.5541	-3.0698	4.6239	1.0190
8	-7.5289	1.6797	9.2086	7.5289	-1.6797	-2.9246	4.6043	0.9288
9	-7.6518	1.5877	9.2395	7.6518	-1.5877	-3.0321	4.6198	0.9950

3.4 ESP analysis

The ESP V(r) is generated by the nuclei and electrons of the molecule in the surrounding space and is defined as follows[30]:

$$V_{tot}(r) = V_{nuc}(r) + V_{ele}(r) = \sum_A \frac{Z_A}{|r-R_A|} - \int \frac{r(r')}{|r-r'|} dr' \quad (4)$$

Z_A is the nuclear charge at the R_A distance of molecule A, and r(r') is the electron density. Multiwfn 3.4.7 software was used to analyze the vander surfaces of molecules[31]. The molecule was analyzed by ESP at the M062X/def2TZVP level. Based on the output file of Multiwfn program, the molecular surface ESP isosurface was rendered by VMD 1.9.3 program[32].

ESP analysis of molecules is not related to reactivity, but it can provide theoretical basis for discussing

molecular interactions. From Fig. 5, the red and blue grid surfaces are positive and negative potentials, respectively. The yellow and green spheres represent extremely high and low points, respectively[33]. The areas are colored in white with potential close to zero. The highest electrostatic potential of the eight molecules is located at H of the carboxyl group, while the highest electrostatic potential is located at C-O double bond of the carboxyl group. The C-C double bond potentials of the four isomeric resinic acids are negative, and the C-C potentials of the allimaric acid are slightly positive. Regions with high electrostatic potential of molecules may interact with highly electronegative parts of other molecules, including solvent molecules.

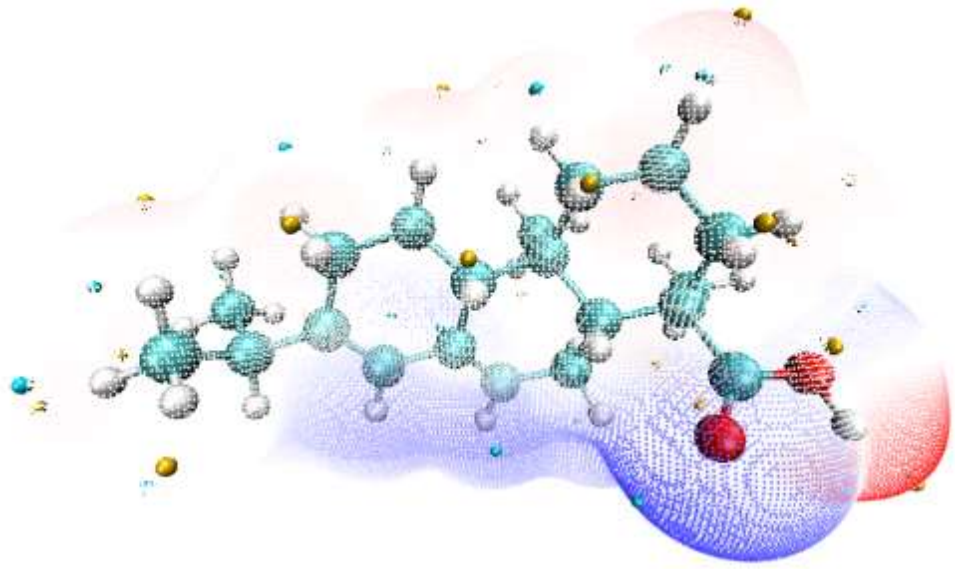

1

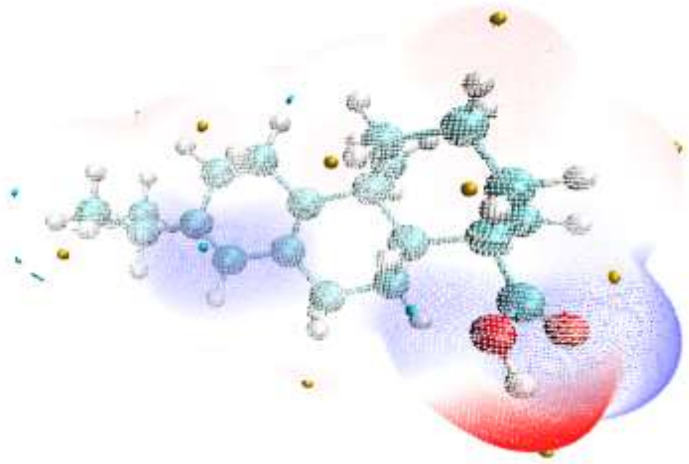

2

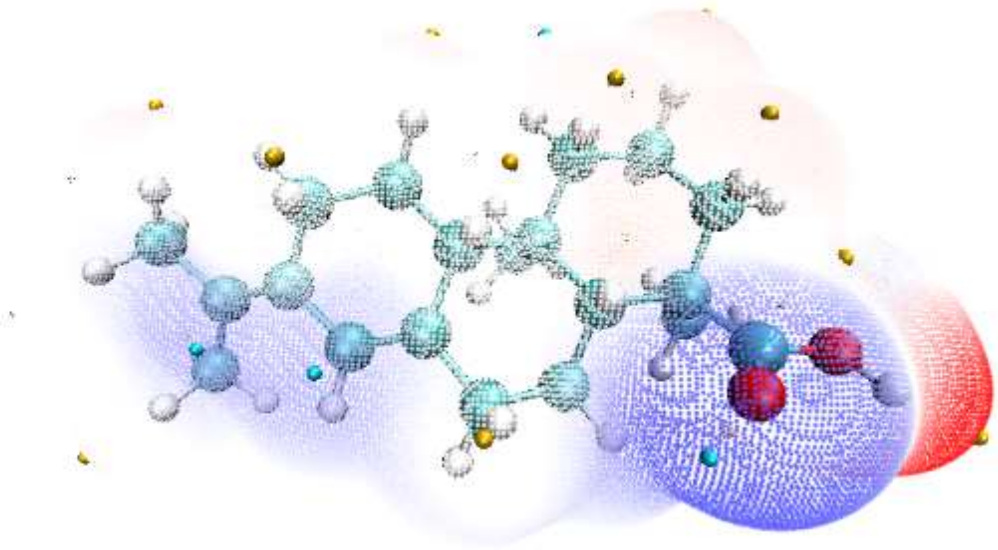

3

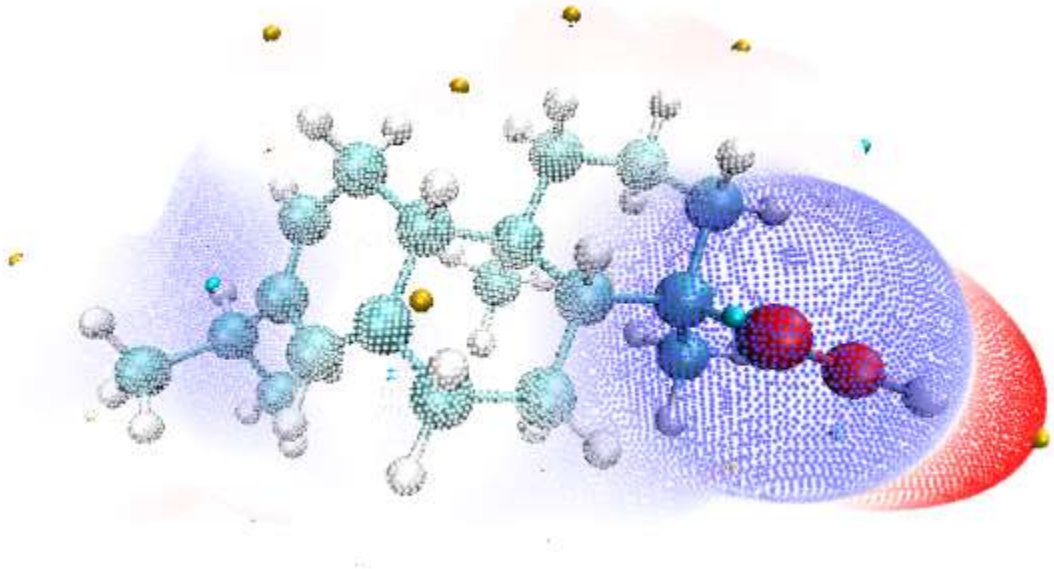

4

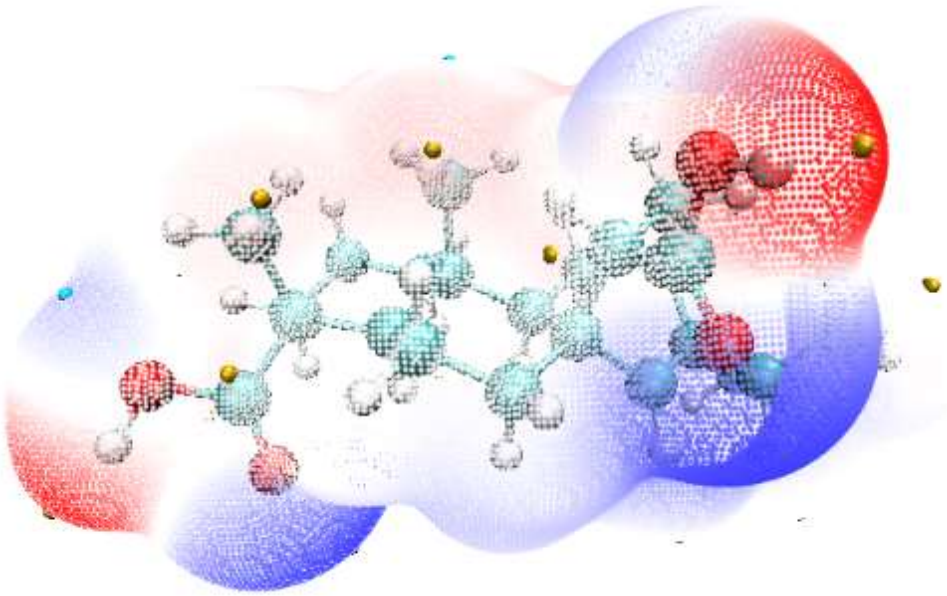

6

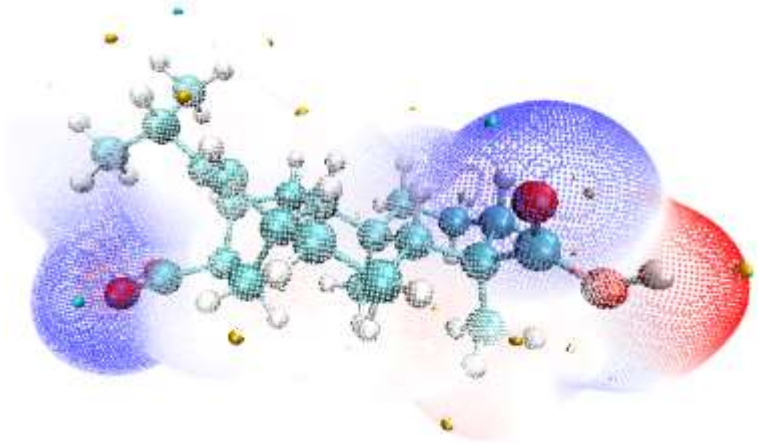

7

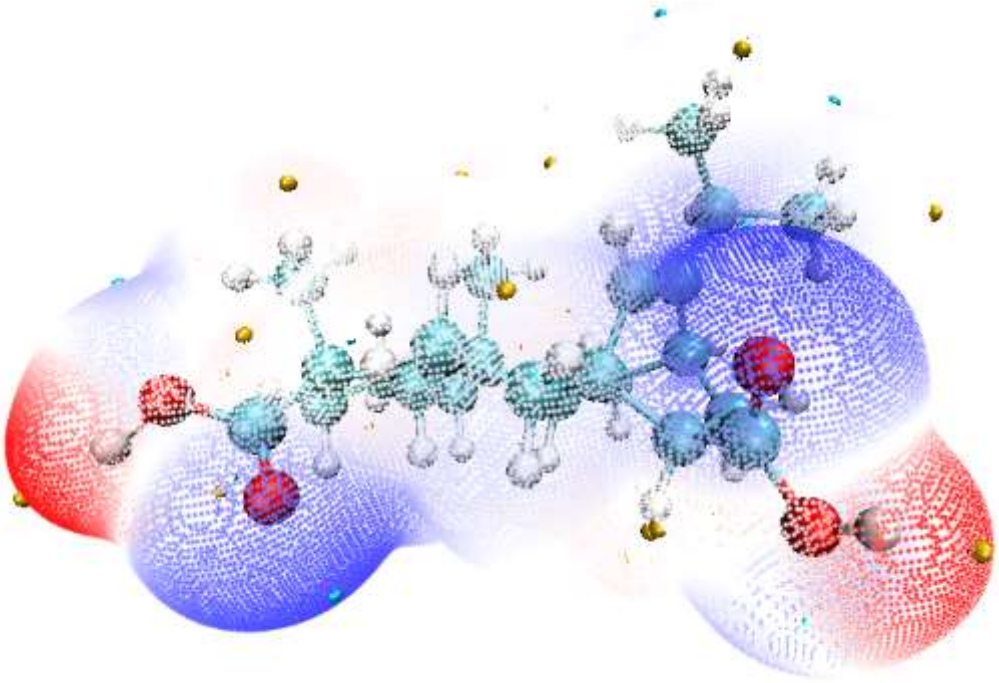

8

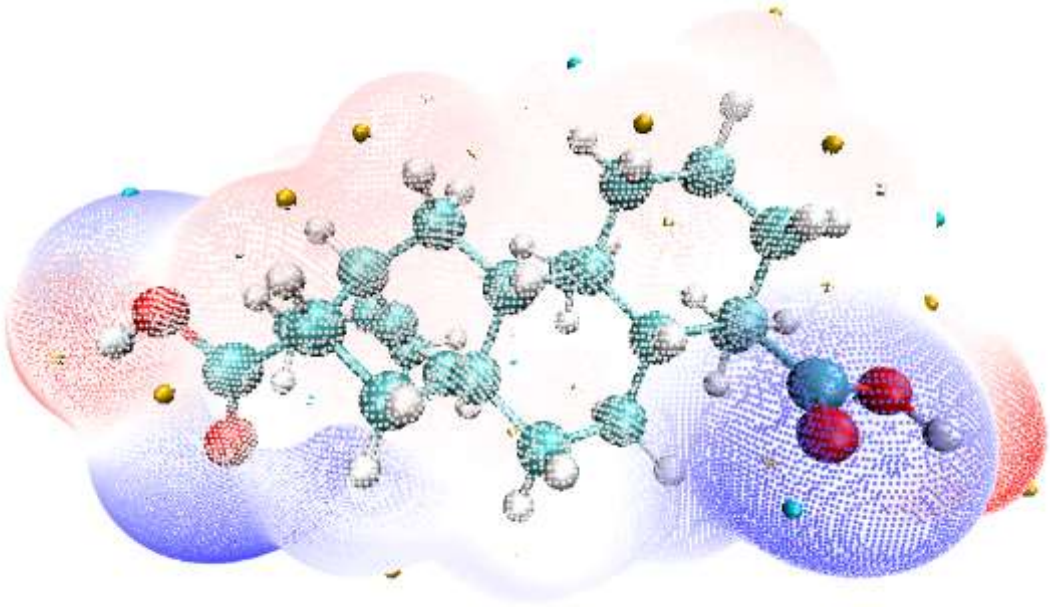

9

Figure 5. ESP of molecules

4 CONCLUSION

Under the protection of nitrogen atmosphere, the resin acids were isomerized to form levopimaric acid(4). Levopimaric acid(4) reacted with acrylic acid through the Diels–Alder reaction to synthesize isomers of acrylopimaric acid. The values of ΔG were sorted from highest to lowest by levopimaric acid(4), neoabietic acid(3), palustric acid(2), and bietic acid(1). The addition reaction of levopimaric acid(4) and acrylic acid(5) to acrylopimaric acid c(8) was the optimal reaction path dynamically. However, ΔG of acrylopimaric acid c(8) was higher than that of acrylopimaric acid d(9). It revealed the reason that levopimaric acid(4) can react with acrylic acid through the

Diels–Alder reaction to form isomers of acrylopimaric acid c(8) and acrylopimaric acid d(9) under microwave heat[6]. The reaction rates k in the addition reaction of levopimaric acid(4) and acrylic acid(5) to acrylopimaric acid in aqueous solution were faster than those of other solvents. Therefore, water is a better solvent for the reactions compared with the other solvents. The active sites of the four isomeric resin acids were the C-C double bonds where the six-member ring is located, and both C-C double bonds are easily attacked by both electrophiles and nucleophiles. For acylpyimaric acid, the non-planar six-memed ring (C53 and C55) and the C-C double bonds were easily attacked by nucleophile, while the non-planar six-memed ring (C9 and C15) and the carboxyl group (O1 and O2) are easily reacted with electrophiles. The highest electrostatic potential of the eight molecules is located at H of the carboxyl group, while the highest electrostatic potential is located at C-O double bond of the carboxyl group. The C-C double bond potentials of the four isomeric resinic acids are negative, and the C-C potentials of the allimaric acid are slightly positive.

Acknowledgements

This research was funded by the National Natural Science Foundation of China (No. 21762006), Specific Research Project of Guangxi for Research Bases and Talents (No. AD18126005), Key R&D Projects of Guangxi Zhuang Autonomous Region (No. AB20238008) and the Scientific Research Foundation of Guangxi University for Nationalities (Project Category: General Project; No. 2020KJYB003).

Not applicable

Funding This research was funded by the National Natural Science Foundation of China (No. 21762006), Specific Research Project of Guangxi for Research Bases and Talents (No. AD18126005), Key R&D Projects of Guangxi Zhuang Autonomous Region (No. AB20238008) and the Scientific Research Foundation of Guangxi University for Nationalities (Project Category: General Project; No. 2020KJYB003).

Conflicts of interest/Competing interests The authors declare that they have no conflict of interest.

Availability of data and material All data generated or analyzed during this work are included in this published article.

Code availability Not applicable

Authors' contributions Wu-ji Lai: Computation, Methodology, Software, Investigation, Writing - Original Draft. Jia-hao Lu: Validation, Formal analysis, Visualization, Software. Rui Jiang: Writing: Review & Editing. Lei Zeng: Writing: Review & Editing. Ai-qun Wu: Writing: Review & Editing. Li-qun Shen: Resources, Writing - Review & Editing.

REFERENCES

[1] Serreqi A N, Gamboa H, Stark K . Resin acid markers for total resin acid content of in-mill process lines of a TMP/CTMP pulp mill[J]. Water Research, 2000, 34 (5): 1727-1733.

[2] Wang H, Liu B, Liu X. Synthesis of biobased epoxy and curing agents using rosin and the study of cure reactions[J]. Green Chemistry, 2008, 10 (11):1190-1196.

[3] Wang Hongxiao, Shang Shibin, Xu Xu. ynthesis of acrylopimaric acid under microwave irradiation[J]. Chemical Engineering Progress, 2011, 7(11):1602-1606.

[4] Bicu I, Mustata F . Polymers from a levopimaric acid-acrylic acid Diels-Alder adduct: Synthesis and characterization[J]. Journal of Polymer Science Part A: olymer Chemistry, 2007, 24 (8): 5979-5990.

[5] Liu X, Xin W, Zhang J. Rosin-derived imide-diacids as epoxy curing agents for enhanced performance[J]. Bioresource Technology, 2010, 7 (9): 2520-2524.

[6] Yanqing Gao, Lingli Li, Hui Chen, Jian Li, Zhanqian Song, Shibin Shang, Jie Song, Zongde Wang, Guomin Xiao. High value-added application of rosin as a potential renewable source for the synthesis of acrylopimaric acid-based botanical herbicides[J]. Industrial Crops & Products. 2015, 78: 131-140.

[7] Ayman M. Atta, Ashraf M. Elsaeed, Reem K. Farag, Shymaa M. El-Saeed. Synthesis of unsaturated polyester resins based on rosin acrylic acid adduct for coating applications[J]. Reactive and Functional Polymers. 2007, 67 (6): 549-563

[8] Liu X, Xin W, Zhang J. Rosin-derived imide-diacids as epoxy curing agents for enhanced performance[J]. Bioresource Technology, 2009, 7 (15): 2520-2524.

[9] Liu, X. Q. Preparation of a bio-based epoxy with comparable properties to those of petroleum-based counterparts[J]. Polymer Letters, 2012, 6 (16): 293-298.

[10] Xie Hui, Shang Shibin, Wang Dingxuan.Synthesis and properties of water-soluble acrylpimaric acid polyester [J]. Chemistry and Industry of Forest Products, 2001, 1 (17): 51-55.

[11] Xie Hui, Cheng Zhi. Preparation of acrylic acid polyurethane coatings [J]. Forest products chemistry and industry, 1998, 3: 67-73.

[12] Zhu Qing, Huang Li, Xie Hui, et al. Synthesis and film properties of UV curable acrylic polyurethane acrylate [J]. Coatings industry, 2009, 1 (10): 44-46.

[13] Kyotani T, Tomita A. Analysis of the Reaction of Carbon with NO/N 2 O Using Ab Initio Molecular Orbital Theory[J]. The Journal of Physical Chemistry B, 1999, 17 (1): 275-278.

[14] Basha S J, Chamundeeswari S, Muthu S. Quantum computational, spectroscopic investigations on 6-aminobenzimidazole by DFT/TD-DFT with different solvents and molecular docking studies[J]. Journal of Molecular Liquids, 2019, 296 (5): 787-797.

[15] Wang M F, Zuo Z J, Ren R P. Theoretical Study on Catalytic Pyrolysis of Benzoic Acid as a Coal-Based Model Compound[J]. Energy & Fuels, 2016, 4 (8): 2833-2840.

[16] Costa R A, Junior E, Lopes G. Structural, vibrational, UV–vis, quantum-chemical properties, molecular docking and anti-cancer activity study of annomontine and N -hydroxyannomontine β-carboline alkaloids: A combined experimental and DFT approach[J]. Journal of Molecular Structure, 2018, 1171 (11): 682-695.

[17] Steven M. Bachrach. Computational organic chemistry[J]. Annual Reports Section 'B' (Organic Chemistry), 2009.

[18] Houk K N, Li Y, Evanseck J D. Transition Structures of Hydrocarbon Pericyclic Reactions[J]. Angewandte Chemie International Edition. 1992, 31: 682-708.

[19] M. J. Frisch, G. B. Trucks, H. B. Schlegel. Gaussian 09, Revision E.01. Wallingford, CT: Gaussian Inc; 2013.

[20] Hratchian H P, Schlegel H B. Using Hessian Updating to Increase the Efficiency of a Hessian Based PredictorCorrector Reaction Path Following Method[J]. Journal of Chemical Theory & Computation, 2005, 1 (3): 61.

[21] Tomasi J, Menucci B, Cammi R. Quantum Mechanical Continuum Solvation Models[J]. ChemInform, 2005, 42 (7): 36.

[22] Yan Z, Truhlar D G. The M06 suite of density functionals for main group thermochemistry, thermochemical kinetics, noncovalent interactions, excited states, and transition elements: two new functionals and systematic testing of four M06-class functionals and 12 other functionals[J]. Theoretical Chemistry Accounts, 2008, 1 (4): 525.

[23] Kelly C P, Cramer C J, Truhlar D G. Aqueous Solvation Free Energies of Ions and Ion−Water Clusters Based on an Accurate Value

for the Absolute Aqueous Solvation Free Energy of the Proton[J]. Journal of Physical Chemistry B, 2006, 110 (32):16066-16081.

[24] Kelly C P, Cramer C J, Truhlar D G. Single-ion solvation free energies and the normal hydrogen electrode potential in methanol, acetonitrile, and dimethyl sulfoxide[J]. Journal of Physical Chemistry B, 2007, 111(2):408-22.

[25] Eyring, Henry. The Activated Complex in Chemical Reactions[J]. Journal of Chemical Physics, 1935, 3(2):107-115.

[26] Tian Lu, TSTcalculator, http://sobereva.com/310

[27] Pearson R G. Chemical hardness and density functional theory[J]. Journal of Chemical Sciences, 2005, 117 (8): 369-377.

[28] Mary Y S, Raju K, Panicker C Y. Molecular conformational analysis, vibrational spectra, NBO analysis and first hyperpolarizability of (2E)-3-phenylprop-2-enoic anhydride based on density functional theory calculations[J]. Spectrochimica Acta Part A Molecular & Biomolecular Spectroscopy, 2014, 131 (5): 471-483.

[29] I. Fleming. Frontier orbitals and organic chemical reactions. John Wiley, London 1976.

[30] Murray JS, Concha MC, Politzer P. Links between surface electrostatic potentials ofenergetic molecules, impact sensitivities and C-NO 2 /N-NO 2 bond dissociation energies. MolPhys 2009;107(1):89–97.

[31] Lu T, Chen F. Multiwfn: a multifunctional wavefunction analyzer. J ComputChem2012;33(5):580–92.

[32] Humphrey W, Dalke A, Schulten K. VMD: visual molecular dynamics. J MolGraphics 1996;14(1):33–8.

[33] Lu T, F Chen. Quantitative analysis of molecular surface based on improved Marching Tetrahedra algorithm[J]. Journal of Molecular Graphics & Modelling, 2012, 38(5):314-323.